

1-1-2014

The Nh2-Hypervariable Region Modulates The Binding Affinity Of Troponin T For Tropomyosin

Chinthaka Kaushalya Amarasinghe
Wayne State University,

Follow this and additional works at: http://digitalcommons.wayne.edu/oa_theses

 Part of the [Biophysics Commons](#), [Molecular Biology Commons](#), and the [Physiology Commons](#)

Recommended Citation

Amarasinghe, Chinthaka Kaushalya, "The Nh2-Hypervariable Region Modulates The Binding Affinity Of Troponin T For Tropomyosin" (2014). *Wayne State University Theses*. Paper 367.

This Open Access Thesis is brought to you for free and open access by DigitalCommons@WayneState. It has been accepted for inclusion in Wayne State University Theses by an authorized administrator of DigitalCommons@WayneState.

**THE NH₂-HYPERVARIABLE REGION MODULATES THE BINDING AFFINITY OF
TROPONIN T FOR TROPOMYOSIN**

by

CHINTHAKA KAUSHALYA AMARASINGHE

THESIS

Submitted to the Graduate School

of Wayne State University,

Detroit, Michigan

in partial fulfillment of the requirements

for the degree of

MASTER OF SCIENCE

2014

MAJOR: PHYSIOLOGY

Approved By:

Advisor

Date

© COPYRIGHT BY
CHINTHAKA KAUSHALYA AMARASINGHE
2014
All Rights Reserved

ACKNOWLEDGEMENTS

I would like to thank my mentor Dr. Jian-Ping Jin for his patience and guidance during my time as a physiology graduate student. I would have definitely not been able to complete my thesis project while developing lifelong critical thinking skills and also mastering a variety of basic science and biochemical techniques without his continued support and helpful feedback. I would also like to thank my colleagues in the lab for their friendship, support and assistance in the lab: Dr. Shirin Akhter, Annie Wang, Dr. Hanzhong Feng, Dr. Md Moazzem Hossain, Dr. Rong Liu, Dr. Bin Wei, and Dr. Hongguang Wei. Last but not least, I would like to thank Christine Cupps for her invaluable help as our department's program assistant. This work was supported by NIH grants AR048816, HL098945 and a WSU OVPR Incubator Grant to Dr. Jian-Ping Jin.

TABLE OF CONTENTS

Acknowledgements.....	ii
List of Tables	vi
List of Figures.....	vii
List of Abbreviations	ix
Chapter 1 - Background.....	1
Structure and Function of Striated Muscle	1
Overall Organization of Striated Muscle Cells	1
Striated Muscle Myofilaments	3
Striated Muscle Contraction	6
Regulation of Striated Muscle Contraction	8
Structure of the Troponin Complex	8
Troponin T.....	10
Molecular Structure and Function	10
Muscle Type Specific Isoforms of TnT.....	12
The N-terminal Hypervariable Region of TnT	13
Hypothesis and Goal of the Present Study	14
Chapter 2 - Methods.....	17
Methodology Overview.....	17
Protein Engineering and Purification	17
Analytical Methods	18
Agarose Gel Electrophoresis.....	18
Sodium dodecyl sulfate polyacrylamide gel electrophoresis (SDS-PAGE).....	19
Western Blot	19

UV and Visible Light Spectrometry	20
Molecular Cloning.....	21
Design of Troponin T Fragments.....	21
Primer Sequences.....	21
Polymerase Chain Reaction (PCR).....	22
DNA Purification.....	23
Phenol/Chloroform Extraction.....	23
Ethanol Precipitation.....	23
Gel Purification of DNA Bands.....	24
Restriction Enzyme Digestion	24
DNA Ligation	24
Bacterial Transformation.....	26
PCR Screening of Transformed Bacterial Colonies	27
Miniexpression and Identification of Recombinant Proteins.....	28
Plasmid Minipreparation.....	30
DNA Sequence Analysis	30
Large Scale Protein Expression and Purification.....	31
Large Scale Expression of Recombinant Troponin T and Fragments.....	31
Ammonium-Sulfate Precipitation	32
Dialysis	33
Column Chromatography.....	34
Anion Exchange Chromatography.....	34
Size-exclusion Chromatography.....	36
Metal Ion Affinity Chromatography.....	37
Lyophilization of Protein.....	39

Tropomyosin Binding Assay	39
Solid-Phase Microplate Protein-Binding Assay	39
Statistical Analysis.....	41
Chapter 3 - Results.....	43
Tropomyosin Binding Affinity of T2 Fragments of Different TnT Isoforms	43
Tropomyosin Binding Affinity of T1 Fragments of Different TnT Isoforms	43
Tropomyosin Binding Affinity of Middle Fragments of Different TnT Isoforms.....	44
Tropomyosin Binding Affinity of Intact TnT Isoforms	45
Tropomyosin Binding Affinity of TnT Comparison within Species and Isoform	45
Chapter 4 - Discussion	47
Methodology and Rationale	47
The Role of TnT's N-Terminal Hypervariable Region in Muscle Fiber-Specific Isoforms	47
Tm Binding Affinity of Sites 1 and 2.....	49
Conclusions	50
References.....	52
Abstract.....	64
Autobiographical Statement.....	66

LIST OF TABLES

Table 1 - Summary of Protein Purification	18
Table 2 - Summary of Protein Binding Experiments	46

LIST OF FIGURES

Figure 1 - Organization of striated muscle	2
Figure 2 - The striated muscle myofilaments	4
Figure 3 – Organization of the skeletal muscle sarcomere.....	5
Figure 4 – Organization of cardiac muscle sarcomere.....	6
Figure 5 – The Cross-bridge cycle.....	8
Figure 6 - The troponin complex	9
Figure 7 – Structure of TnT isoforms	11
Figure 8 – Sequence alignment of Tm binding sites 1 and 2 across TnT isoforms.....	12
Figure 9 - Evolutionary lineage of TnT isoforms	13
Figure 10 – TnT constructs used in this study	16
Figure 11 - General biochemical techniques used in this study.....	17
Figure 12 - PCR construction of McTnT T2 cDNA from full length McTnT cDNA	22
Figure 13 – Plasmid map of pAED4.....	25
Figure 14 – Plasmid map of pTX3.....	25
Figure 15 - PCR screening of transformed bacterial colonies	28
Figure 16 – SDS-PAGE and Western blot of the expression of MsTnT	33
Figure 17 – DE52 anion exchange column purification of MsTnT.....	36
Figure 18 – G75 Size exclusion column purification of MsTnT	37
Figure 19 – SDS-PAGE and Western blot of Zn ²⁺ affinity column purification of Tx3-MfTnT middle fragment.....	39
Figure 20 - ELISA-based solid-phase protein binding assay.....	42
Figure 21 – No significant differences in Tm binding affinity between T2 fragments across isoforms.	43
Figure 22 – Significant differences in Tm binding affinity between T1 fragments across isoforms.	44

Figure 23 - No significant differences in Tm binding affinity between middle fragments across isoforms.	44
Figure 24 - Significant differences in Tm binding affinity between intact TnT isoforms.	45
Figure 25 – Comparison of Tm binding affinity of intact, T1, T2 and middle fragments of cardiac TnT	46
Figure 26 – A model summarizing the findings	51

LIST OF ABBREVIATIONS

ADP	Adenosine diphosphate
Amp	Ampicillin
ATP	Adenosine triphosphate
bp	Base pair
BSA	Bovine serum albumin
cDNA	Complimentary DNA
Chl	Chloramphenicol
CNBr	Cyanogen bromide
cTnC	Cardiac troponin C
cTnI	Cardiac troponin I
cTnT	Cardiac troponin T
ddH₂O	Double-distilled water
dNTP	Deoxynucleotide
dsDNA	Double stranded DNA
EDTA	Ethylenediaminetetraacetic acid
EGTA	Ethylene glycol tetraacetic acid
ELISA	Enzyme-linked immunosorbent assay
EtBr	Ethidium bromide
F-actin	Fibrous actin
fTnT	Fast TnT
G-actin	Globular actin
HRP	Horseradish peroxidase
IPTG	Isopropyl β -D-1-thiogalactopyranoside

McTnT	Mouse cardiac troponin T
MfTnT	Mouse fast troponin T
NC	Nitrocellulose
PCR	Polymerase chain reaction
Pi	Inorganic phosphate
PMSF	Phenylmethylsulfonyl fluoride
RT	Room temperature
SDS	Sodium dodecyl sulfate
SDS-PAGE	Sodium dodecyl sulfate polyacrylamide gel electrophoresis
sTnT	Slow troponin T
TAE	Tris-acetate-EDTA
TBE	Tris-borate-EDTA
TBS	Tris-buffered saline
TE	Tris-EDTA
Tm	Tropomyosin
TnC	Troponin C
TnI	Troponin I
TnT	Troponin T

CHAPTER 1

BACKGROUND

Structure and Function of Striated Muscle

Muscle is a contractile tissue that is responsible for a variety of body movements via the ability to convert ATP into mechanical energy (Marieb & Hoehn, 2013). There are three types of muscle: skeletal, cardiac and smooth muscle. Around 40% of the human body mass is skeletal muscle while another 10% is smooth and cardiac muscle (Hoyle, 1969; Hall & Guyton, 2011). Skeletal muscle is attached to the skeleton and primarily responsible for voluntary movement. Cardiac muscle is primarily found in the heart where it constitutes the majority of the chamber walls. Smooth muscle is found in hollow visceral organs such as the stomach, the urinary bladder and the vasculature, and plays a role in the facilitation of fluid and substance motility (Hall & Guyton, 2011).

Both skeletal muscle and cardiac muscle are classified as striated muscle, due to the visible striations under a light microscope (A. F. Huxley & Niedergerke, 1954; H. Huxley & Hanson, 1954; Hanson, 1968). To give a background of my thesis study, this chapter will focus on striated muscle and the function of troponin T (TnT) in the regulation of striated muscle contraction.

Overall Organization of Striated Muscle Cells

Striated muscle consists of myocytes or muscle fibers, which are in turn comprised of myofibrils. These myofibrils contain contractile units called sarcomeres that consist of myofilaments including the actin thin and myosin thick filaments. The actin thin filaments and myosin thick filaments overlap and are integrated together in an array to comprise the sarcomere (Figure 1). During contraction and relaxation of muscle, the actin and myosin filaments slide along each other to alter lengths of the sarcomere (H. E. Huxley, 1990). Under

the light microscope, dark anisotropic bands (A-bands) occur where the thin and thick filaments overlap. Light isotropic bands (I-bands) solely consist of thin filaments are present in areas of non-overlapping with the thick filaments. Both the A and I bands repeat along the length of the myofibril to create the visible striations under the light microscope (A. F. Huxley & Niedergerke, 1954; H. Huxley & Hanson, 1954; Hanson, 1968; Marieb & Hoehn, 2013).

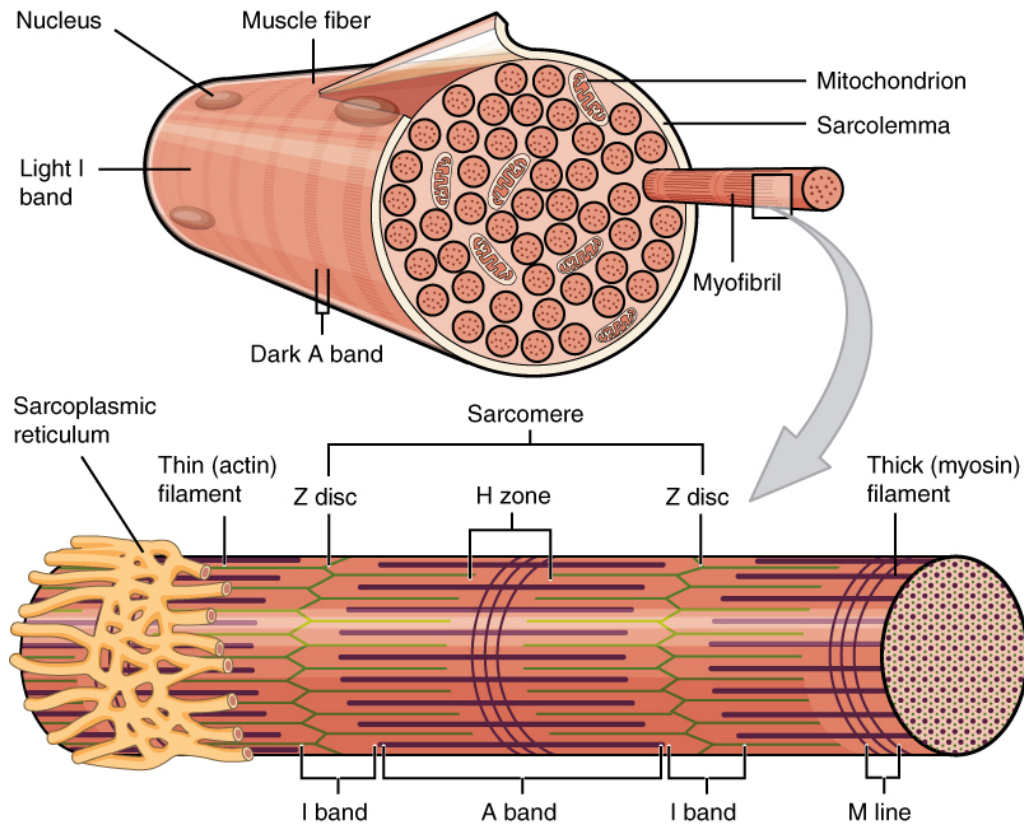


Figure 1 - Organization of striated muscle (OpenStax College, CC BY-SA 3.0)

The thick filaments contain myosin and extend the entire length of the A band (Figure 1) while the thin filaments containing actin extend the length of the I-band, and also partly into the A-band. The Z-disc (Z-lines), mostly comprised of alpha-actinin, defines the border of the individual sarcomeres, and is responsible for anchoring the thin filaments (H. Huxley & Hanson, 1954; Ebashi & Ebashi, 1965; Maruyama & Ebashi, 1965; Hanson, 1968; Hall & Guyton, 2011).

Striated Muscle Myofilaments

Contraction of striated muscle relies on the interactions of the thin and thick filaments. Thick filaments are around 16 nm in diameter and contains around 300 myosin molecules. Each myosin molecule consists of four light and two heavy polypeptide chains, and contains three domains: the head, neck and tail (Figure 2). The head domain binds to the actin in the thin filament to form a cross-bridge, will allows force generation via ATP hydrolysis. The neck domain of myosin associates with several light-chain regulatory subunits and the tail domain affects the specific function of myosin within cells (Gazith, Himmelfarb, & Harrington, 1970; Marieb & Hoehn, 2013).

The thin filament is primarily composed of actin. This 42 kDa protein is found in the thin filament as globular actin (G actin,) which polymerizes to form two intertwined of fibrous actin (F actin). F actin is comprised of approximately multiple actin monomers (Hanson & Lowy, 1963; Holmes, Popp, Gebhard, & Kabsch, 1990; Herman, 1993), Tropomyosin (Tm) and the troponin complex are also proteins located within the thin filament that are involved in striated muscle contraction. Tropomyosin is a rod-shaped molecule containing a 40 nm coiled units of two parallel dimeric chains, similar to that of a myosin tail. Tropomyosin is almost always found physiologically as a dimer, and these dimers may comprise of different tropomyosin isoforms. Muscle tissue usually contains α/β heterodimers with the exception of cardiac muscle that expresses only a single α -Tm isoform (Gimona, Watakabe, & Helfman, 1995). The two strands of tropomyosin molecules run diametrically opposed along the actin filaments and help stiffen and stabilize the thin filament. Each tropomyosin dimer is in contact with seven actin units and are arranged end to end along the actin filaments (Figure 2). In a relaxed muscle fiber, they block the myosin-binding sites on actin so that myosin heads on the thick filaments cannot bind to the thin filaments (Ebashi & Ebashi, 1965; Marieb & Hoehn,

2013).

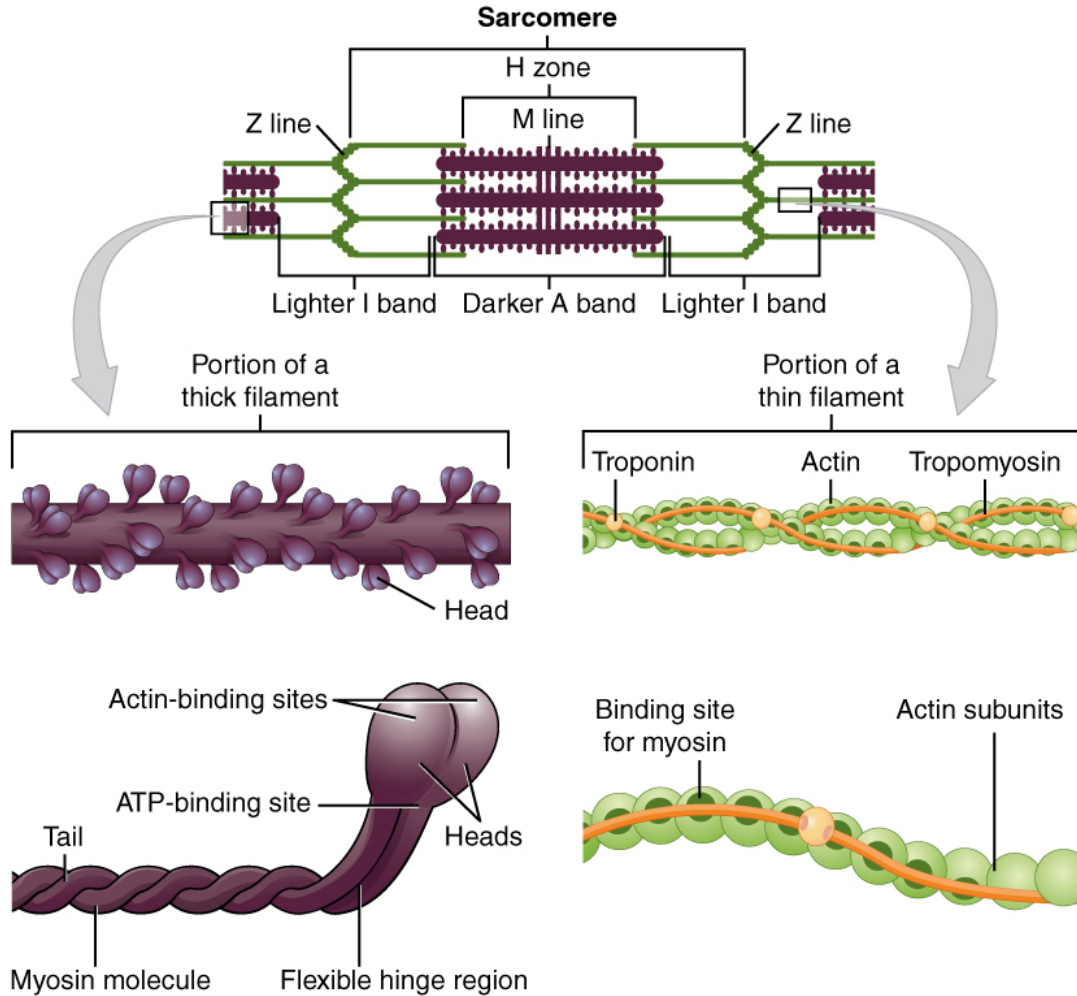


Figure 2 – The striated muscle myofilaments (OpenStax College, [CC BY-SA 3.0](#))

Titin is a giant protein around 3000 kDa that connects the Z line to the M line in the sarcomere (Figures 3 & 4) (K. Wang, McClure, & Tu, 1979; Horowitz, Kempner, Bisher, & Podolsky, 1986). Titin's role is to function as a molecular spring and scaffold by regulating the sarcomere tension via contributing to the overall passive tension in striated muscle (Horowitz et al., 1986; Linke et al., 1997; Jin, 2000; Sanger & Sanger, 2001). Titin is modular in structure as around 90% of its mass consists of repeating fibronectin-III and immunoglobulin-C2 domains and which provide binding sites for a variety of myofibrillar proteins, such as actin, α -actinin, myosin, telethonin, myosin binding protein-C, myomesin, and obscurin (Pfuhl & Pastore, 1995;

Rief, Gautel, Schemmel, & Gaub, 1998; Sanger & Sanger, 2001) .

Nebulin is another giant protein (600-900 kDa) only found in skeletal muscle (Figure 3) that associates with the thin filament (Horowitz et al., 1986; K. Wang & Wright, 1988). Nebulin is mostly comprised of 35 residue repeats that allows a tight association with the thin filament via a central consensus sequence of SDxxYK (Jin & Wang, 1991). Each actin polymer is associated with two nebulin molecules, with each nebulin filament spanning the length of the actin monomer within the thin filament. Nebulin binds to other actin-associated proteins such as tropomyosin, which indicates that nebulin is well integrated into the thin filament. Nebulin's close association with the thin filament allows it to stabilize the thin filament and modulate thin filament length (K. Wang & Wright, 1988; Jin & Wang, 1991; Ogut, Hossain, & Jin, 2003; Castillo, Nowak, Littlefield, Fowler, & Littlefield, 2009). In cardiac muscle, nebulinette (Figure 4) is an 800 kDa protein that exhibits high homology with nebulin and fulfills similar roles such as sarcomere assembly and contractile function (Moncman & Wang, 1995; Ogut et al., 2003).

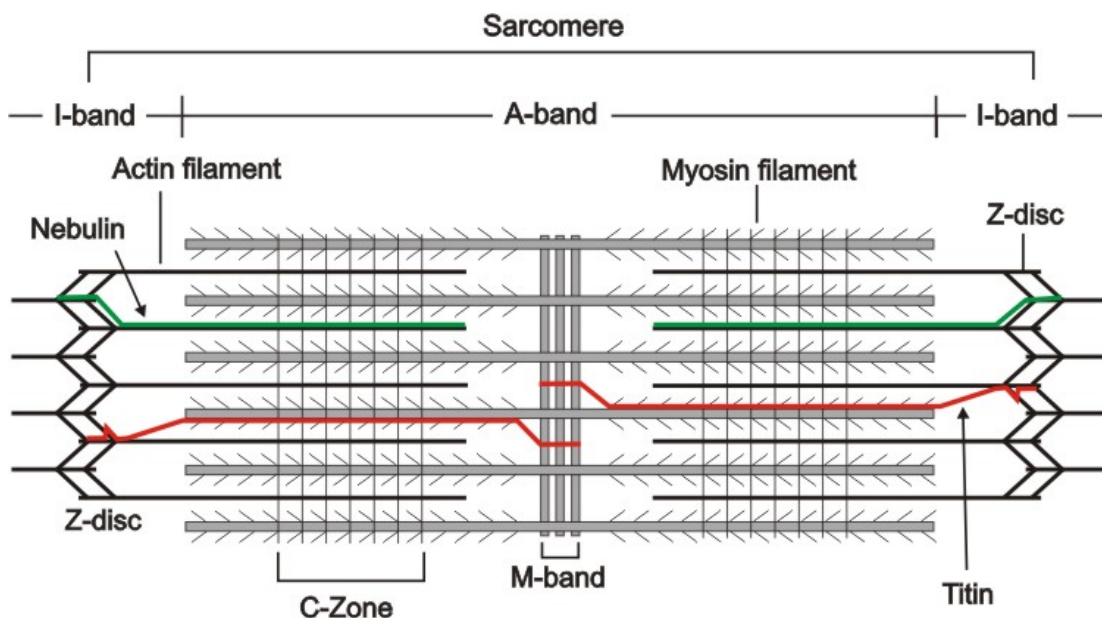


Figure 3 - Organization of the skeletal muscle sarcomere. Retrieved from http://www.pradeepluther.com/pklwork19may02/images/Sarcomere_diagram.jpg

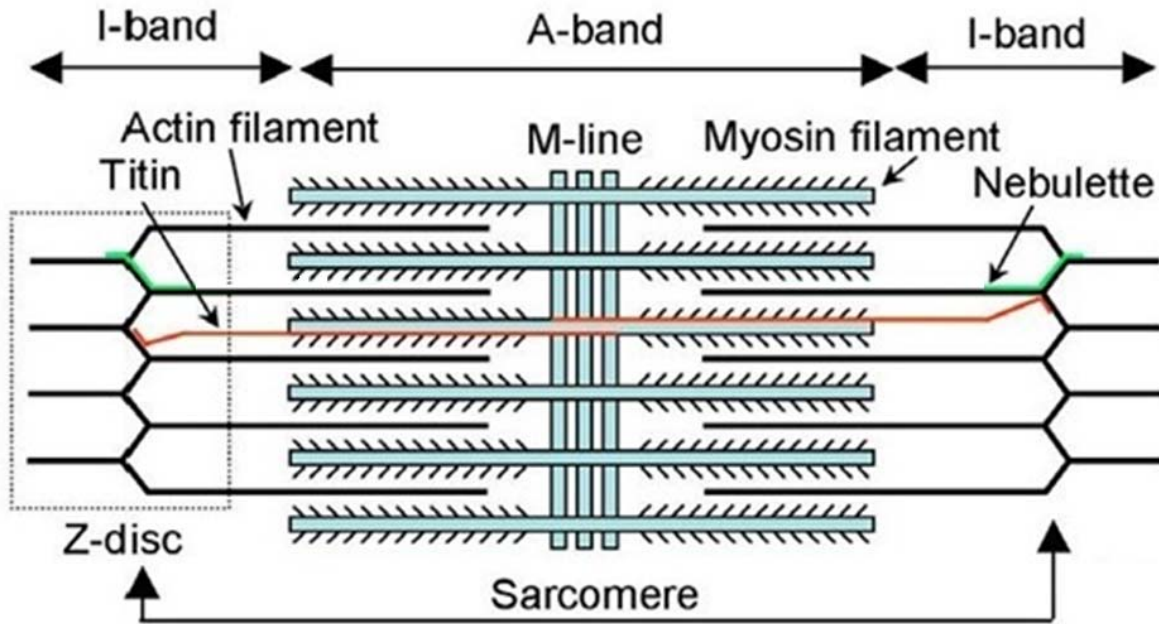


Figure 4 - Organization of the cardiac sarcomere, modified from (Veselka, 2012).

Striated Muscle Contraction

In 1954, the molecular basis of muscle contraction was described by two groups: A. F. Huxley and R. Niedergerke and H. E. Huxley and J. Hanson (A. F. Huxley & Niedergerke, 1954; Hoyle, 1969). Their findings described the relative positions of myosin and actin filaments during various stages in muscle contraction, and how these interactions resulted in the production of contractile force. Under the microscope, it was shown that the length of the A-band does not change during muscle contraction. However, it was found that the I-band, rich in actin thin filaments, changed its length along with the sarcomere (A. F. Huxley & Niedergerke, 1954; H. Huxley & Hanson, 1954). Based on these observations, the sliding filament theory was developed, which proposes that the sliding of actin past myosin generates muscle tension. Since the actin thin filaments are anchored to the Z-disc, shortening of the thin filament results in increased overlapping of the thin and thick filaments and subsequent shortening of the sarcomere, which ultimately results in the shortening of the muscle (Hoyle, 1969).

Muscle contraction on the molecular level occurs when the myosin head on the thick

filament attaches to an actin filament to form a cross-bridge (Figure 5). Then, the myosin head rotates toward the myosin tail, which pulls on the thin filament, causing the thin filament to move relative to the thick filament (power stroke). The myosin head detaches and rotates back to the initial orientation, completing one cross-bridge cycle. This process is coupled with ATP hydrolysis catalyzed by the ATPase activity of the myosin head during its interaction with actin in the thin filament (Ebashi & Ebashi, 1965; Vale & Milligan, 2000; Volkmann & Hanein, 2000; Goody, 2003).

When striated muscle is relaxed, the cross-bridges are unattached and the myosin heads on the thick filaments are at a 90 degrees angle in regards to the thin filaments (Figure 5, step 2). In this relaxed state, the myosin head is ATP-bound. When intracellular Ca^{2+} increases upon the stimulation of muscle contraction, Ca^{2+} binds to troponin and induces a conformational change in tropomyosin, which exposes the myosin binding sites on the actin thin filaments (Ebashi, 1963; Potter & Gergely, 1974; Zot & Potter, 1987). The myosin head is then able to weakly bind to the actin thin filament to form a cross-bridge (Figure. 5, step 3). The inorganic phosphate is then released in order to facilitate a strong attachment between actin and myosin. Because of this strong attachment, the myosin heads rotate at a 45 degree angle towards actin (Figure 5, step 4), generating a force on the thin filaments which results in the thin filaments to slide relatively to the thick filaments to generate the power stroke. Next, ADP disassociates from the myosin head and the subsequent binding of ATP causes the cross-bridge to detach (Fig 5, step 1) (Hall & Guyton, 2011; Marieb & Hoehn, 2013). Hydrolysis of ATP to ADP and Pi by the myosin-ATPase returns the myosin head's orientation to 90 degrees relative to the thin filament (Figure 5, step 2). This cycle is repeated as long as the intracellular Ca^{2+} concentration remains sufficiently elevated (Goody, 2003).

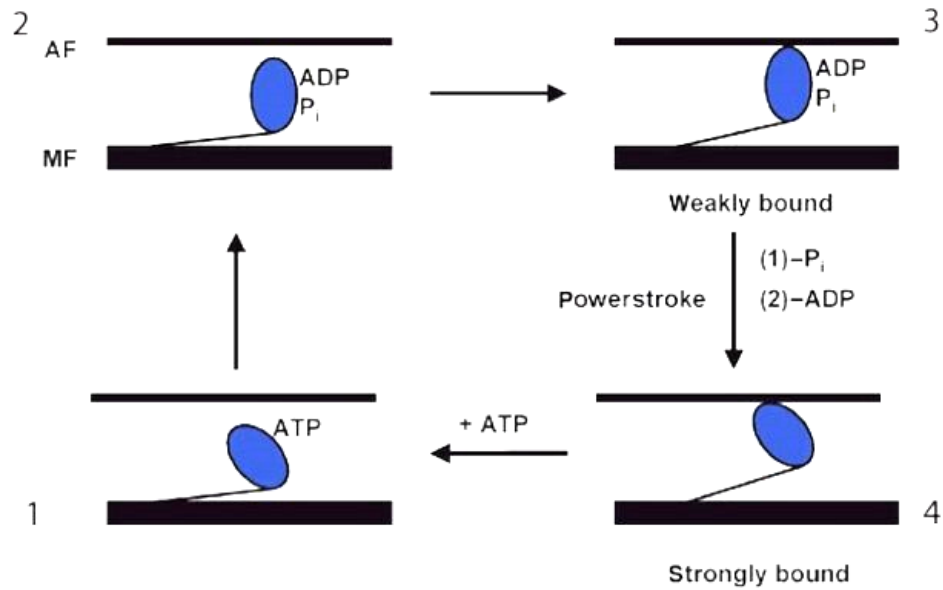


Figure 5 – The Cross-bridge cycle (Goody, 2003). AF: Actin filament, MF: Myosin filament

Regulation of Striated Muscle Contraction

Striated muscle contraction is regulated by intracellular Ca^{2+} concentration via the thin filament regulatory proteins, i.e., the troponin complex and tropomyosin. In the absence of intracellular Ca^{2+} , the interaction of myosin with actin is inhibited due to the unexposed myosin binding sites on the actin thin filaments. After the intracellular Ca^{2+} concentration increases due to Ca^{2+} release from the sarcoplasmic reticulum, Ca^{2+} binds to the troponin complex, which reconfigures the position of tropomyosin and exposes the myosin binding sites on the actin thin filament, allowing the binding of the myosin head to actin to initiate cross-bridge cycling (Gomes, Potter, & Szczesna-Cordary, 2002; Goody, 2003).

Structure of the Troponin Complex

By the 1960's Ebashi and colleagues identified a mixture of proteins that induced muscle relaxation when the mixture and ATP was added to muscle fibers (Ebashi, 1963; Ebashi & Endo, 1968; Potter & Gergely, 1974; Zot & Potter, 1987; Endo, 2008). This relaxing factor was later discovered to be the proteins that make up the troponin complex. The troponin complex

consist of three protein subunits: Troponin C (TnC), the calcium sensor, Troponin I (TnI), which binds to actin, and Troponin T (TnT), which anchors the troponin complex to tropomyosin (Figure 6). The overall role of troponin is to regulate the contraction and relaxation of striated muscle. When the muscle is relaxed, TnI is bound to actin and blocks the myosin binding sites on actin (Drabikow.W & Nonomura, 1968; Spudich, Huxley, & Finch, 1972; Drabikow.W, Nowak, Barylko, & Dabrowsk.R, 1973; Vaneerd & Kawasaki, 1973; Dabrowska, Nowak, Podlubnaya, & Drabikowski, 1975). Thus, TnI-actin interactions are a regulatory mechanism to prevent cross-bridge formation and subsequent muscle contraction (Nakaoka, 1972; Yamamoto & Maruyama, 1973; Dabrowska, Podlubnaya, Nowak, & Drabikowski, 1976; Dowben, Ford, & Bunting, 1976). Upon an increase in intracellular Ca^{2+} , Binding of Ca^{2+} to TnC leads to a conformation change between the switch region of TnI and a hydrophobic patch in TnC's N-terminal region. This interaction between TnI and TnC releases TnI's inhibition of cross-bridge formation by pulling TnI's inhibitory region away from actin and consequently allowing the myosin head to bind to actin (Gomes, Potter, et al., 2002; Goody, 2003; Endo, 2008).

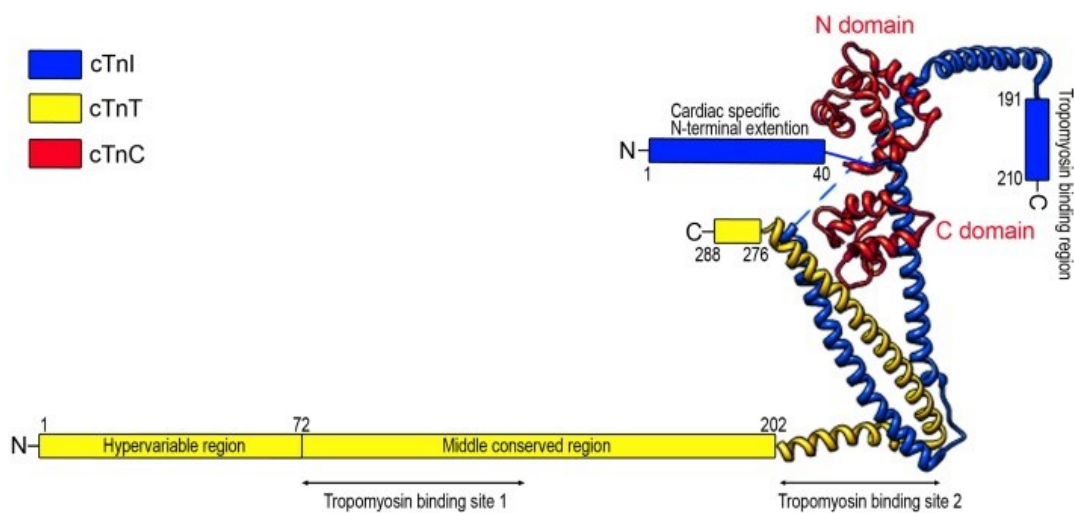


Figure 6 – The troponin complex (Sheng & Jin, 2014)

Troponin T

Molecular Structure and Function

Troponin T is a 30-35 kDa protein whose difference in size can be attributed to the variable length of the N-terminal region. Even though a basic function of TnT is to anchor the troponin complex to tropomyosin, the variable structure of TnT across isoforms has various physiological and pathological implications in muscle function (Schachat, Diamond, & Brandt, 1987; Pan & Potter, 1992; Anderson et al., 1995; Fisher, Wang, & Tobacman, 1995; Briggs & Schachat, 1996; Watkins, Seidman, Seidman, Feng, & Sweeney, 1996; J. Wang & Jin, 1998; Huang, Brozovich, & Jin, 1999; Jin, Chen, Ogut, & Huang, 2000; Zhang, Biesiadecki, & Jin, 2006; Biesiadecki, Chong, Nosek, & Jin, 2007). TnT is present in vertebrates in slow skeletal, fast skeletal and cardiac muscle isoforms with greatest variation in the N-terminal region across isoforms (Figure 7) (Hoyle, 1969; Mak & Smillie, 1981; Leavis & Gergely, 1984; Jin & Lin, 1988). TnT's rather conserved C-terminal region contains binding sites for TnC, TnI, and Tm while the also conserved middle region contains a binding site for tropomyosin (site 1) (Mak & Smillie, 1981; Leavis & Gergely, 1984; Morris & Lehrer, 1984; Heeley, Golosinska, & Smillie, 1987; Zot & Potter, 1987; Jin & Chong, 2010).

Several decades ago, it was demonstrated that chymotrypsin treatment results in two TnT fragments named T1 (equivalent to the cyanogen bromide (CNBr) cleaved fragment CB1) and T2 that each contain a tropomyosin binding site (Pearlstone, Carpenter, & Smillie, 1977; Mak & Smillie, 1981; Morris & Lehrer, 1984; Heeley et al., 1987). The T1 fragment containing site 1 consists of amino acids 2-158 in rabbit fast skeletal muscle TnT while the T2 fragment containing site 2 consists of amino acids 159-259. T1 region tropomyosin binding site has been further localized (Figure 8) to amino acids 117–143 in mouse cardiac TnT (exon 10) and 72–97 in rabbit fast TnT (exon 11).

Since there is limited crystal structure data only pertaining to TnT's C-terminal region, TnT's two binding sites have only been recently mapped out (Takeda, Yamashita, Maeda, & Maeda, 2003; Jin & Chong, 2010). In previous literature, TnT's Tm binding site on the C-terminal region has been hypothesized to be located on the very end of the C-terminal. However, this assertion has not been supported by experiments showing that deletion in the very C-terminal end does not significantly affect Tm binding or ATPase activity (Jha, Leavis, & Sarkar, 1996; Jin, Chong, & Hossain, 2007). Rather, the T2 region binding site has recently been localized to amino acids 180–204 in slow TnT (exon 11), and 174-198 in rabbit fast skeletal muscle (exon 14), which indicates that the T2 region binding site is actually located towards the beginning of the T2 region (Figure 6 & 8). Both the middle and the T2 Tm binding sites are highly conserved muscle-fibre specific cross isoforms (Jin & Chong, 2010).

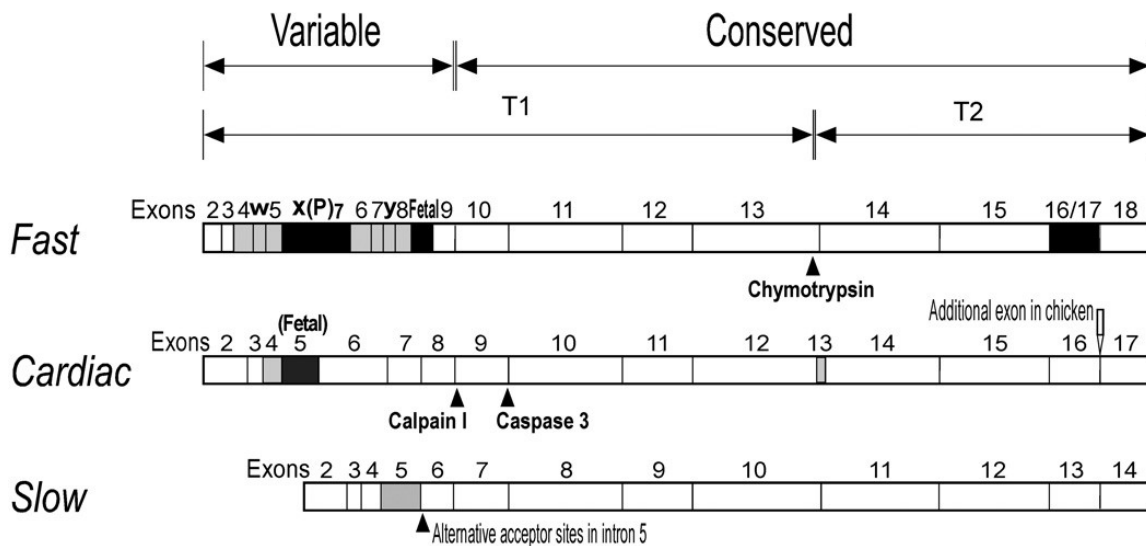


Figure 7 – Structure of TnT isoforms. The TnT isoforms has a conserved core region and C-terminal region with the greatest difference in the N-terminal region (Jin & Chong, 2010)

Figure 8 – Sequence alignment of Tm binding sites 1 and 2 across TnT isoforms. Both Tm binding sites are highly conserved. The numbers of homologous exons encoding these segments are shown in the background while identical or conserved residues encoded by the two Tm-binding sites main coding exons are outlined with the gray bars above the sequences (Jin & Chong, 2010)



Muscle Type Specific Isoforms of TnT

TNNT1, *TNNT2*, and *TNNT3* are three homologous genes of TnT that encode respectively the slow, cardiac and fast isoforms of TnT. These TnT isoforms are expressed specifically in their respective muscle fibers in a non-redundant manner (Cooper & Ordahl, 1985; Breitbart & Nadalginaud, 1986; Anderson et al., 1995; Jin, Chen, & Huang, 1998), as it has been shown that knockout of the cardiac TnT gene results in embryonic lethality (Nishii et al., 2008). The three muscle fiber-type specific TnT isoforms have the greatest diversity in their N-terminal hypervariable region (Figure 7). It is important to note that the diversity of TnT isoforms is greater across isoforms than that within the same isoform across species (Figure 9) (Verin & Gusev, 1988; Mesnard et al., 1995; Chandra, Kim, & Solaro, 1997; Jin & Root, 2000; Gomes, Guzman, Zhao, & Potter, 2002; Feng, Biesiadecki, Yu, Hossain, & Jin, 2008; Chong & Jin, 2009). This feature suggests that the N-terminal hypervariable region has a muscle fiber-specific role in regulating the function of TnT, and consequently, the function of specific muscle fiber types.

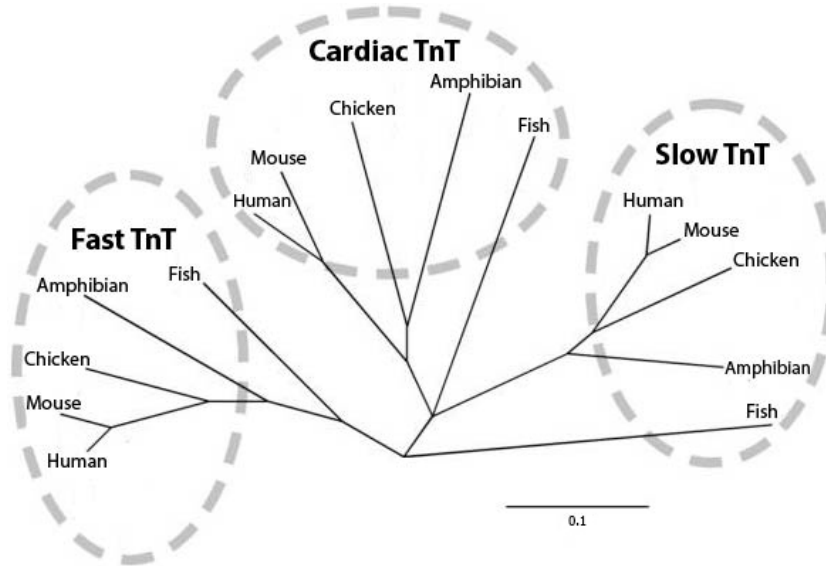


Figure 9 - Evolutionary lineage of TnT isoforms. Sequence divergence show that TnT isoforms vary greater across isoforms than between species. The evolutionary distances are indicated with a ruler bar for the rate of amino acid substitution (Modified from Chong & Jin, 2009)

The N-terminal Hypervariable Region of TnT

TnT's N-terminal hypervariable region does not bind to any other thin filament proteins and its absence does not abolish the binding of TnT to tropomyosin. Deletion of the N-terminal region from cardiac TnT has been observed not to abolish but to increase TnT's overall binding affinity for tropomyosin, suggesting that the N-terminal region is a regulatory structure of TnT (Verin & Gusev, 1988; Pan, Gordon, & Potter, 1991; Jin et al., 2000; Jin & Root, 2000; Biesiadecki et al., 2007; Feng et al., 2008). Furthermore, it has been observed that the N-terminal variable region in TnT is regulated by alternate RNA splicing during muscle development and other physiological conditions, which suggests that the modulatory structure of the N-terminal region is a site that regulates muscle function via the modulation of TnT's structure and function (Breitbart et al., 1985; Cooper & Ordahl, 1985; Breitbart & Nadalginard, 1987; Gahlmann, Troutt, Wade, Gunning, & Kedes, 1987; Jin, Huang, Yeh, & Lin, 1992; Akella, Ding, Cheng, & Gulati, 1995; Anderson et al., 1995; Briggs & Schachat, 1996; Wei & Jin, 2011).

Alternate splicing of the N-terminal variable region during muscle development has been

shown to alter force production in skinned fibers and aberrant splicing of this region has been correlated with various cardiomyopathies such as dilated cardiomyopathy and other cardiac dysfunctions (Jin & Lin, 1988; Anderson et al., 1995; Wei & Jin, 2011; Feng, Chen, Nan, Huang, & Jin, 2014). Alternate splicing of fast TnT (fTnT) has been observed to generate acidic and basic isoforms of TnT with significantly different binding affinities to Tm and TnI, indicating that the charge of the N-terminal region contributes to the TnT's overall binding to Tm and TnI (J. Wang & Jin, 1997; Ogut, Granzier, & Jin, 1999; Biesiadecki et al., 2007). Because the N-terminal region is able to alter TnT's binding to TnI and Tm, of which the binding sites are remotely located, it was hypothesized that the N-terminal region might affect the overall conformation of TnT. This hypothesis was supported by epitope analysis data showing that alterations in the N-terminal region is propagated to the core and C-terminal regions (J. Wang & Jin, 1998; Jin et al., 2000). Even though it is known that the N-terminal region can modulate TnT's binding affinity to Tm, it is still unclear to what extent and how each of TnT's tropomyosin binding sites contribute to the overall binding affinity to Tm.

Hypothesis and Goal of the Present Study

Although TnT's C-terminal domain and middle region is very much conserved, the N-terminal region is hypervariable (Figure 7), and varies significantly across isoforms and plays a modulatory role in the Ca^{2+} regulation of muscle contraction. The N-terminal region contributes to the fine-tuning of Ca^{2+} regulation of contractility, as it has been observed that the activity of myosin ATPase varies across TnT isoforms despite the conserved core structure of TnT (Gomes, Guzman, et al., 2002). An unresolved discrepancy in the literature shows variable differences in tropomyosin binding when comparing the T1 and T2 fragments of different TnT isoforms. The fast TnT T1 fragment has been shown to have greater or equal affinity for Tm compared to the fast TnT T2 fragment, while the slow TnT T1 has been observed to have a

significantly lower binding affinity to Tm compared to slow TnT T2 (Pearlstone & Smillie, 1982; Heeley et al., 1987; Jin & Chong, 2010). This discrepancy in the literature may be attributed to the modulatory function of the N-terminal region that is variable among muscle-fiber specific isoforms. The N-terminal hypervariable region of TnT may affect the affinity of tropomyosin binding sites 1 and 2 across isoforms by changing the overall molecular conformation, as it is already known that there are differences in binding site affinity across isoforms despite conserved core structure. To investigate this hypothesis in this thesis study, TnT fragments will be engineered, expressed and purified, and tropomyosin binding affinity will be evaluated in enzyme-linked immunosorbent assay (ELISA)-based solid phase protein binding experiments. Understanding to what extent the N-terminal hypervariable region's structure affects the affinities of the tropomyosin binding sites of TnT will deepen and further our understanding of how conformational changes in TnT affect tropomyosin-thin filament interactions, thus modulating contractile properties of striated muscle under a variety of physiological and pathological conditions.

The overall goal of this thesis project is to compare the tropomyosin binding affinities of intact TnT and TnT fragments from different muscle fiber-specific isoforms to understand the effect of the N-terminal region on tropomyosin binding affinity of the middle binding site of T1 (site 1). This study will also be able to explain the previous discrepancies in the literature that show variable Tm binding affinities of the T1 fragments when compared to their respective T2 fragments (Pearlstone & Smillie, 1982; Heeley et al., 1987; Jin & Chong, 2010). To investigate this issue, five sets of tropomyosin binding assays will be conducted, comparing intact TnT, T1 and T2 fragments across muscle fiber specific isoforms, as well as N-terminal truncated T1 fragments (middle fragments) across isoforms to examine the tropomyosin binding affinity of site 1 without the influence of the N-terminal region. The last binding assay set will compare

intact TnT and the various TnT fragments within the same isoform and same species in order to understand how the intrinsic affinity of each Tm binding site differs within the same protein as well as the effect of the N-terminal hypervariable region on site 1. The intact TnT and TnT fragments studied in the present research are summarized in Figure 10.

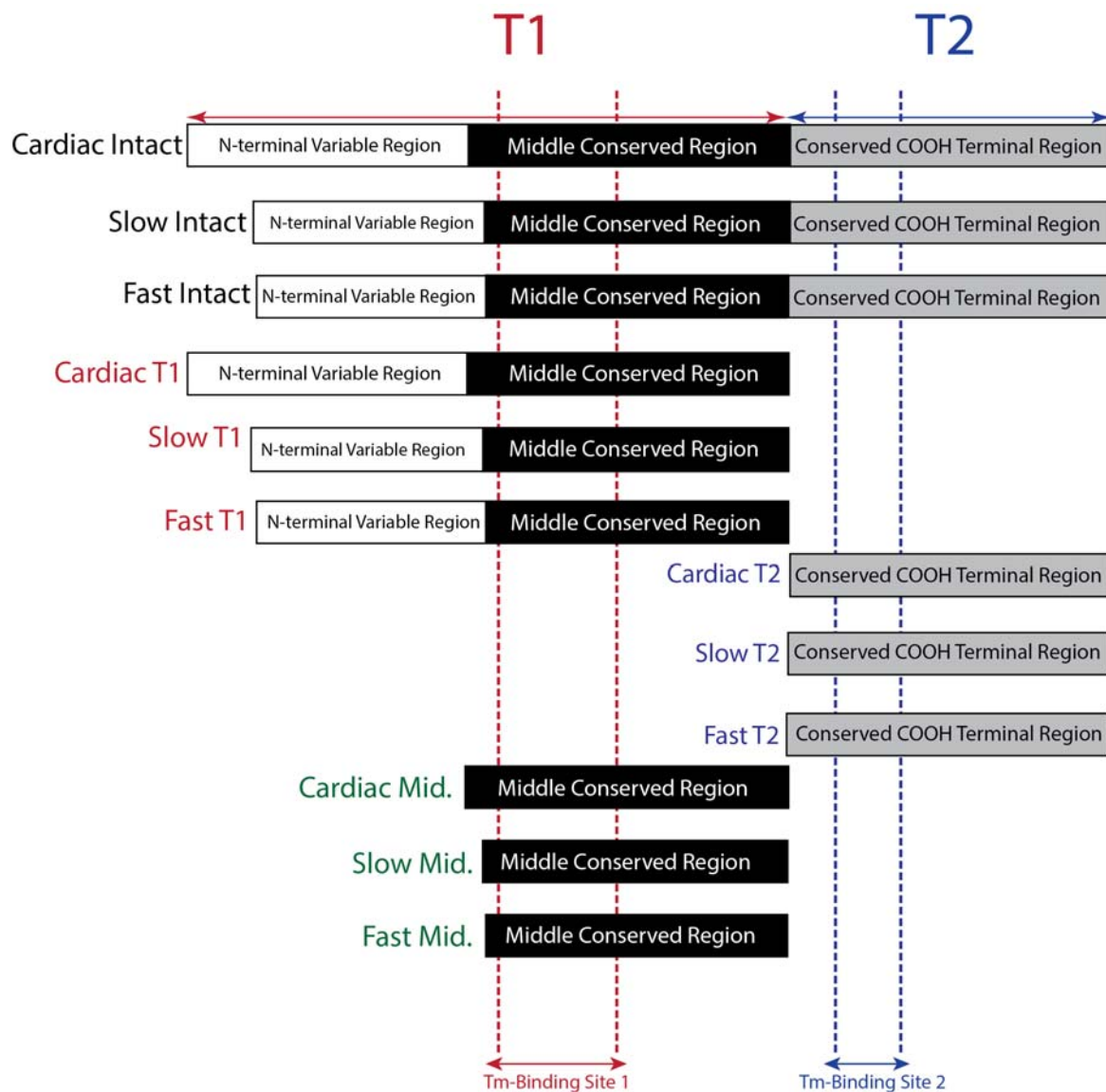


Figure 10 – TnT constructs used in this study

CHAPTER 2

METHODS

Methodology Overview

To meet the goals of this thesis project, a variety of basic science and biochemical techniques are employed (Figure 11). In order to understand the Tm binding affinities within the intact TnTs and TnT fragments, vectors expressing the coding cDNA were generated, and proteins were purified from transformed bacterial cultures using various chromatographic techniques. The protein preparations were verified for their authenticity and used in solid-phase microtiter plate assays to examine their binding affinities to Tm.

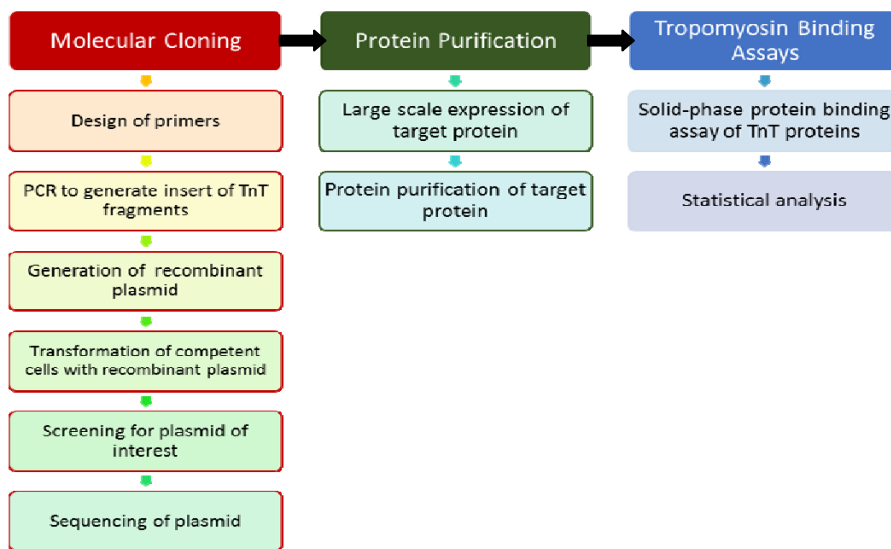


Figure 11 – General biochemical techniques used in this study

Protein Engineering and Purification

The purification steps for each protein used in this study are described below. Some protein preparations were previously made in Dr. Jin's laboratory and available for the present study while some needed further purification. For some of the proteins, there was no engineered coding cDNA available and therefore the insert was generated using recombinant polymerase chain reaction (PCR) from cDNA template and then cloned into a vector for protein

expression (Table 1).

Table 1 – Summary of Protein Purification

Intact TnT			
TnT Protein	Mouse Cardiac	Mouse Slow	Rabbit Fast
Techniques Used	Already available	<ul style="list-style-type: none"> • Bacterial expression • Ammonium sulfate precipitation • Anion exchange chromatography (DE52) • Size exclusion chromatography (G75) 	<ul style="list-style-type: none"> • Size exclusion chromatography (G75) of impure protein fraction
TnT T1 Fragments			
TnT Protein	Mouse Cardiac T1	Human Slow T1	Rabbit Fast T1
Techniques Used	<ul style="list-style-type: none"> • Primer design for PCR amplification of insert from intact cDNA • Cloning into insert • Bacterial expression • Ammonium sulfate precipitation • Affinity chromatography 	Already available	Already available
TnT Middle Fragments			
TnT Protein	Mouse Cardiac Middle	Mouse Slow Middle	Mouse Fast Middle
Techniques Used	<ul style="list-style-type: none"> • Primer design for PCR amplification of insert from intact cDNA • Cloning into insert • Bacterial expression • Ammonium sulfate precipitation • Affinity chromatography 	Already available	<ul style="list-style-type: none"> • Primer design for PCR amplification of insert from intact cDNA • Cloning into insert • Bacterial expression • Ammonium sulfate precipitation • Affinity chromatography
TnT T2 Fragments			
TnT Protein	Mouse Cardiac T2	Mouse Slow T2	Rabbit Fast T2
Techniques Used	<ul style="list-style-type: none"> • Primer design for PCR amplification of insert from intact cDNA • Cloning into insert • Bacterial expression • Ammonium sulfate precipitation • Affinity chromatography 	Already available	Already available

Analytical Methods

Agarose Gel Electrophoresis

Agarose gels were casted and run in Tris-Borate-EDTA (TBE) buffer, with a final concentration of 0.34 mcg/mL ethidium bromide (EtBr). Based on the size of the DNA to be visualized on the gel, different concentrations of agarose was used in order to obtain the most

optimum resolution. For linear double stranded DNA (dsDNA) 800 to 12,000 base pairs (bp), 0.6% (w/v) gels were casted, and for dsDNA 500-10,000 bp, 200-3,000 bp, 1% (w/v) and 1.5% (w/v) agarose were used, respectively. Samples were loaded after adding bromophenol blue tracking dye and glycerol to a final concentration of 10% and the gel was run at a constant voltage of 5-10V/cm in a horizontal tank.

Sodium dodecyl sulfate polyacrylamide gel electrophoresis (SDS-PAGE)

SDS-PAGE was used with a Bio-Rad mini-gel system for the analysis of protein samples. 14% resolving gels containing acrylamide/bis-acrylamide at the ratio of 180:1 were used to resolve proteins of 30 kDa or greater and 12% gels containing acrylamide/bis-acrylamide at the ratio of (29:1) were used to resolve proteins 10-30 kDa for optimum separation of protein bands. Protein samples were homogenized in SDS-PAGE sample buffer containing 2% SDS. After being heated at 80°C for 5 min, the samples were clarified by spinning in a Beckman Coulter Microfuge 18 at 14,000 rpm (14,539 x g) at room temperature (RT) for 5 min. The samples were then loaded into the gel and the gels were run with a constant current of 25 mA/0.75 mm of SDS-PAGE gel. After running, the gel was fixed and stained in Coomassie Brilliant Blue R250 in 50% methanol and 10% acetic acid for 45 minutes and destained in 10% acetic acid to reveal the resolved protein bands.

Western Blot

Nitrocellulose (NC) membrane, thin and thick filter papers were soaked in transfer buffer (Tris-glycine buffer and 20% methanol) for 30 minutes on an orbital shaker at 65 rpm. After the SDS-PAGE gels finished running, the gel was placed in a “transfer sandwich” (thick/thin filter paper-gel-NC membrane-thin/thick filter paper, from top to bottom) in a Bio-Rad Laboratory semidry electrotransfer apparatus. The current limit was set to 5 mA per cm² and the maximum voltage was set to 25 V during the 15 minutes of transfer.

The membrane was then incubated in blocking buffer (1% bovine serum albumin (BSA) Tris-buffered saline (TBS)) at room temperature for 30 minutes on a rocker. After blocking, the membrane was incubated with the appropriate primary antibody diluted in TBS containing 0.1% BSA at a pre-tested concentration on a rocker at 4°C overnight.

After the primary antibody incubation, the membrane was washed 3 times in TBS containing 0.5 Triton X-100 and 0.1% SDS at 80 rpm on a rotator for 7 minutes per wash. The membrane was then washed 2 times with TBS for 3 minutes per wash. After the washing step, the membrane was placed in TBS containing 0.1% BSA with the final concentration of 1:10,000 of alkaline phosphatase conjugated goat anti-mouse IgG second antibody at RT on the rotator for 50 min. After second antibody incubation, the above washing procedure was repeated.

For development of the substrate reaction, 10 mL of alkaline phosphatase buffer with 5-Bromo-4-chloro-3-indolyl phosphate (3.3 mg/mL) and Nitro blue tetrazolium was used to develop the membrane at room temperature in a cardboard box to avoid light exposure. The membrane was developed until the target protein band was clearly seen but not oversaturated (optimally 10-15 min).

For visualization of agarose gels, a UV transilluminator was initially used to confirm optimal separation. After good separation, the gels were again placed on the UV transilluminator and photographed with a 2 second exposure time using a FinePix S7000 camera.

UV and Light Spectrometry

For visible and UV light spectrometry, two different spectrophotometers were used. A BioRad SmartSpec spectrophotometer was used to quantify the absorbance of bacterial cultures at OD₆₀₀. 1 mL of growth media before inoculation was used a blank for baseline control and 1 mL of bacterial culture was used to monitor bacterial growth during large scale protein purification. For estimation of protein concentrations, a Beckman Coulter DU 520

spectrophotometer was used. A Beckman Coulter microcell containing 100 μ L of 1x ELISA buffer (see ELISA protocol) for baseline control. Then, the protein in 1x ELISA buffer was loaded into a clean microcell and then scanned with the spectrophotometer across wavelengths. The absorbance value at 280 nm was recorded, and the concentration of the protein was calculated using the Beer-Lambert law by using the calculated extinction value obtained from the ExPASy database (Artimo et al., 2012).

Molecular Cloning

Design of Troponin T Fragments

DNA sequences of the mouse cardiac TnT (McTnT) T1, McTnT T2, mouse fast TnT (MfTnT) middle and McTnT middle fragments were amplified from their respective intact complementary DNA (cDNA) sequences. To obtain the coding cDNA fragment, forward and reverse PCR primers were constructed flanking the target sequence. The forward primer contained an NdeI restriction enzyme cutting site and a Met initiation codon and the reverse primer contained a stop codon prior to an EcoRI restriction site to facilitate the ligation of the insert into the expression vector. The primers were synthesized at Integrated DNA Technologies.

Primer Sequences

McTnT T1:

Forward: 5' CA CAT ATG TCK GAC VYV GAR GAR GWG GTG G 3'
NdeI

Reverse: 5' CTC TGT CTT GAA TTC TCA CCC TCC AAA GTG 3'
EcoRI Stop

McTnT T2

Forward: 5' CC AAC CAT ATG CAC TTT GGA GGG TA 3'
NdeI

Reverse: 5' G AGA ATT CTA YTT CCA RCG YCC GGT GAC 3'
EcoRI Stop

McTnT middle:

Forward: 5' AG CCC CAT ATG CTC TTC ATG CCC AAC TT 3'
 NdeI

Reverse: 5' CTC TGT CTT GAA TTC TCA CCC TCC AAA GTG 3'
 EcoRI Stop

MfTnT middle:

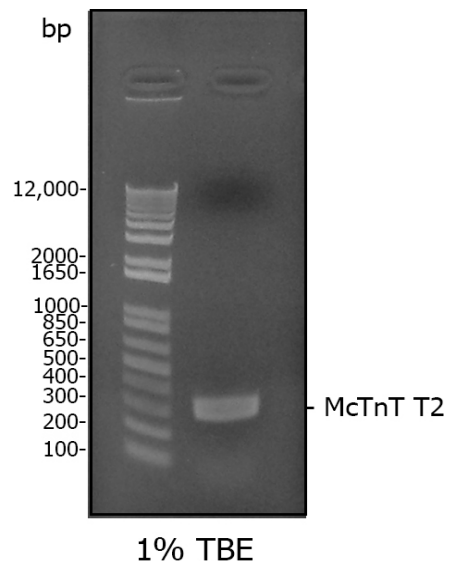
Forward: 5' AGA CCC AAA CAT ATG GCT CCT AAG A 3'
 NdeI

Reverse: 5' C AGC CTT GAA TTC TCA GCT GCT GTA 3'
 EcoRI Stop

Polymerase Chain Reaction (PCR)

PCR was used to amplify the cDNAs encoding TnT fragments from full length cDNAs of TnT. Each reaction tube contained a final concentration of the following in Millipore ddH₂O: 10 fmol/ μ L of the forward and reverse primer, 0.1 mM dNTP, and 20 pg/ μ L of the plasmid DNA template. The amount of DNA polymerase used consisted of 90% Taq DNA polymerase and 1 unit total of 10% *pfu* DNA polymerase with proofreading activity (Agilent), to reduce the rate of PCR-introduced random mutations. PCR runs of 25 cycles were carried out in an Applied Biosystems 2720 Thermal Cycler. The initial denaturation time at 95°C was 4 min using hot start, and each PCR cycle consisted of denaturation at 95°C for 20 s, annealing at 55°C for 30 s and extension at 72°C for 1 min. PCR products were purified using the methods detailed in the later section "DNA Purification".

Figure 12 - PCR construction of McTnT T2 cDNA from full length McTnT cDNA



DNA Purification

In order to ensure subsequent successful restriction enzyme digestion and vector ligation, PCR inserts and vectors were purified after restriction enzyme digestion using the following methods:

Phenol/Chloroform Extraction

Phenol/chloroform extraction was used to inactivate and denature any protein impurities after PCR or restriction enzyme digestion. Phenol:chloroform:isoamyl alcohol was made in a 25:24:1 ratio with a pH of 7.9 and the bottom organic layer was mixed with the DNA solution in a 1:1 ratio. The mixture was vortexed at top speed for 20 s and then centrifuged in a Beckman Coulter Microfuge 18 at 14,000 rpm (14,539 x g) at RT for 2 min. The DNA containing clear aqueous phase on top was collected using a pipette and transferred into a new tube.

Ethanol Precipitation

EtOH precipitation was used to further purify and concentrate the cDNA insert or vector. 3M NaOAc, pH 5, was added to the DNA at 10% of the original volume. EtOH was added to the mixture at 2.5x the volume of the NaOAc-DNA mixture. The tube was then chilled for 10 min in dry ice and then centrifuged in a Beckman Coulter Microfuge 18 at 14,000 rpm (14,539 x g) at 4°C for 10 min. The supernatant was discarded and the pellet that contained the DNA was washed with 100-200 µL of 75% EtOH without disturbing the pellet. The tube was then centrifuged again as above for 2 min and the supernatant was discarded. The pellet containing the DNA was allowed to air dry for 30 min and the pellet was resuspended in an appropriate volume of TE buffer (10 mM Tris-HCl and 1 mM ethylenediaminetetraacetic acid (EDTA)).

Gel Purification of DNA Bands

To isolate the DNA product of interest, DNA bands isolated as agarose gel slices were extracted and recovered with glass bead absorption using the Prep-A-Gene system in order to remove any unwanted DNA and other impurities. DNA was resolved in Tris-acetate-EDTA (TAE) agarose gel via electrophoresis at $5\text{V}/\text{cm}^2$. After electrophoresis, the gel was visualized under a long wavelength UV transilluminator and the DNA band of interest was cut out using a clean razor blade. The agarose gel piece was suspended in Prep-A-Gene binding buffer and then melted in a 50°C water bath. After the gel piece was melted, glass beads were added to absorb the DNA. The subsequent washes of the beads with binding and washing buffers, and the elution of purified DNA were carried out according to the manufacturer's protocol.

Restriction Enzyme Digestion

Restriction enzyme digestion was used to cut the expression vectors and inserts to generate compatible sticky ends to facilitate the insertion of the PCR inserts of cDNA encoding TnT fragments into the expression vector. Double digestion of the insert or vector was carried out in the digestion buffer for NdeI (NEB), with 10 units each of NdeI (NEB) and EcoRI (NEB) per μg of DNA at 37°C for 4 hr. The mixture was then purified using the methods detailed in the Section of "DNA Purification".

DNA Ligation

Insert and vector ligation was carried out in a 3:1 molar ratio of insert:vector, in T4 ligase buffer (NEB) using $1\ \mu\text{L}$ T4 ligase (NEB) per $10\ \mu\text{L}$ total reaction volume. The ligation mixture was incubated overnight at 16°C . The ligation mixture was then used to transform (see Bacterial Transformation section) JM109 competent *E. coli* cells in order to produce ampicillin-resistant colonies containing the expression vector of interest with high fidelity. These colonies were later screened using PCR for the presence of expression vector of interest.

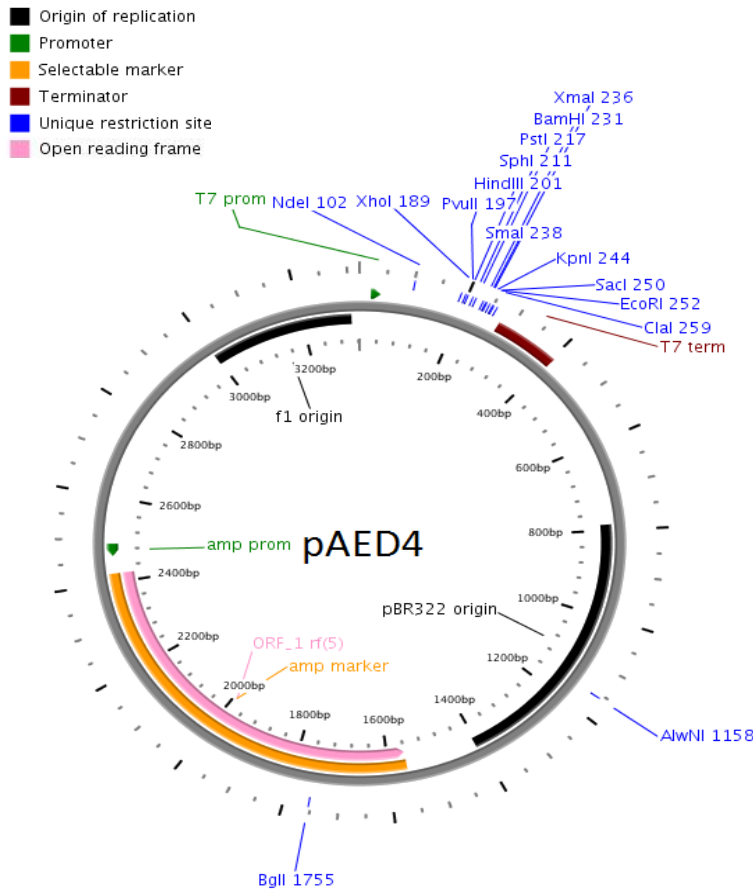
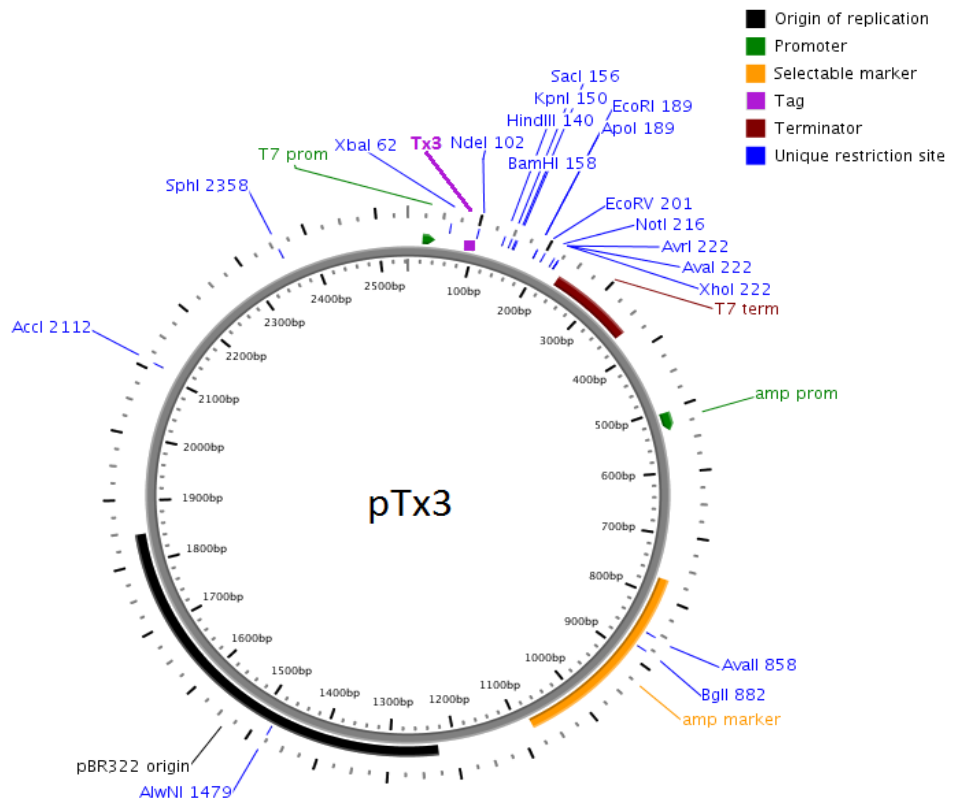


Figure 13 – Plasmid map of pAED4. pAED4 was used to express and purify untagged proteins

Figure 14 – Plasmid map of pTx3. pTx3 was used to purify poorly expressed proteins with the aid of the N-terminal Tx3 (HEEAHHEEAHHE EAH) affinity tag



Bacterial Transformation

Transformation of JM109 or BL21 (DE3)pLysS competent *E. coli* cells with DNA was used for a variety of purposes such as:

1. *E. coli* K12 JM109 capable of replicating target plasmid with high fidelity that could be used for cloning the cDNA constructs followed by PCR colony screening and plasmid minipreparation.
2. BL21(DE3)pLysS containing target plasmid for recombinant protein expression (Studier & Moffatt, 1986).
3. BL21(DE3)pLysS expressing target protein for subsequent inoculation into culture media for large scale protein expression and purification.

An aliquot of competent cells was put on ice until just thawed. 20 ng or more of recombinant plasmid DNA was added to the aliquot and the mixture was swirled with the tip of the pipet. The solution was then incubated on ice for 30 min. The tube was heat shocked at 42°C for 90 s to facilitate uptake of plasmid into the cell, and then put back on ice for 2 min. Using proper sterile technique, LB media was added to the tube at 3-folds or more of the volume of the cell-DNA mixture and incubated at 37°C on a rotary shaker for 45 min. During this time, the respective Luria-Bertani Broth (LB) plate was taken out of storage and warmed up in a 37°C incubator. For the transformation of JM109 cells, LB plates containing 100 µg/mL ampicillin (amp) was used for selection since the pET/pAED4 vectors used in this study contained an ampicillin resistance gene (ampR). For transformation of BL21(DE3)pLysS, LB plates containing 100 µg/mL amp and 12.5 µg/mL chloramphenicol (chl) were used for double selection since pLysS plasmid contained an additional chloramphenicol resistance gene (chlR). After the 45 min. incubation, the bacteria culture was spread evenly on the LB plate and put into the 37°C incubator. After drying out the visible liquid, the LB plate was flipped, with the lid

facing down to avoid desiccation. The plate was then incubated at 37°C overnight for bacterial growth.

PCR Screening of Transformed Bacterial Colonies

After ampicillin selection of the transformed JM109 cells, individual colonies were smeared onto 100-mm LB plate containing 100 µg/mL ampicillin, divided into ~20 separate quadrants, one for each colony and incubated at 37°C for 6 hr. Next, a sterile toothpick was used to lightly scrape a small area of the colony smear, and then dipped into a PCR tube containing 15 µL of a Jin lab-made Redmix PCR mix solution added with specific PCR primers at final concentrations of 10 fmol/µL each. To screen for the recombinant plasmid containing a specific cDNA insert by PCR, one flanking primer was placed in the vector and used together with the other flanking primer in the target cDNA (Figure 15A). This strategy ensures that colonies positive with a PCR amplified band indicate the presence of recombinant plasmid containing the specific vector-insert pair (Figure 15B). The PCR steps were identical to those mentioned in the 'PCR' section.

After PCR, the Redmix PCR products were directly loaded into a TBE agarose gel and then visualized to identify colonies that had a band corresponding to the amplification of the fragment generated by the correct vector-insert combination. Using a sterile toothpick, ~1/3 of a positive bacterial smear was picked up and dipped into extraction solution consisting 20 µl each of phenol:chloroform:isoamyl alcohol and TE buffer. The mixture was vortexed at top speed for 2 s and then centrifuged in a Beckman Coulter Microfuge 18 at 14,000 rpm (14,539 x g) at RT for 2 min. The DNA in the clear aqueous phase was examined with agarose gel as above or pipetted out and transferred into a new tube for use in the transformation of BL21 cells for mini-protein expression screening (Figure 15B).

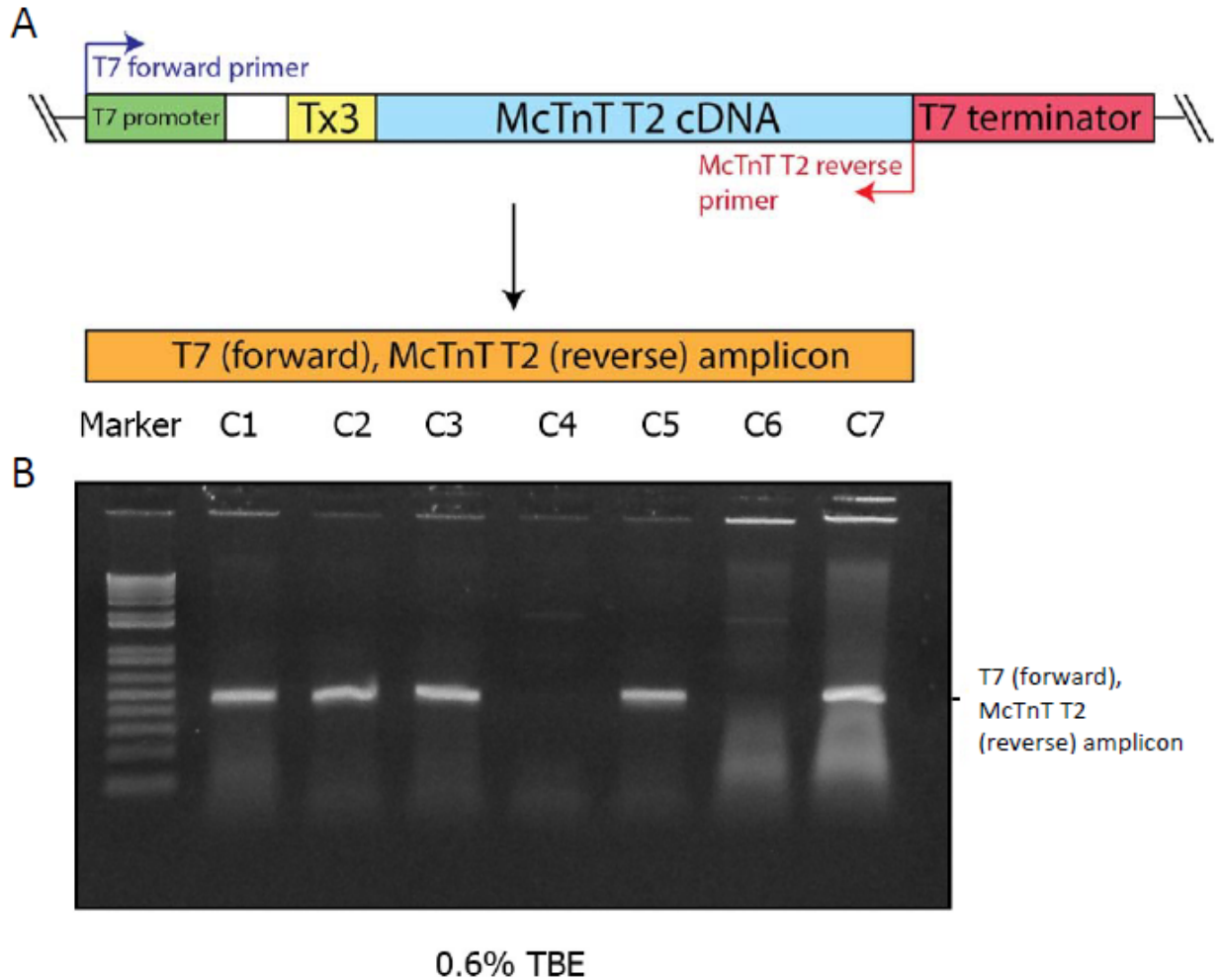


Figure 15 – PCR screening of transformed bacterial colonies. (A): Linear map of the DNA amplified from the pTx3-McTnT T2 plasmid. (B): Colony PCR screening of 7 colonies, 5 which contain the plasmid of interest.

Miniexpression and Identification of Recombinant Proteins

Phenol:chloroform:isoamyl alcohol extracted DNA from positive JM109 colonies was used to transform BL21(DE3)pLysS competent cells in order to verify expression of the target protein. The competent BL21(DE3)pLysS cells were transformed in a similar manner as that described in the ‘Bacterial Transformation’ section with some modifications. A stock of 200 μL competent cells was divided into 6 aliquots and each transformed with 1 μL of phenol:chloroform:isoamyl alcohol extracted DNA from different positive colonies. The tubes were incubated on ice for 30 min and the tubes were then heat shocked at 42°C for 25 s instead

of 90 s to account for the small volume. The addition of LB media and the incubation of the cells were carried out as above in a standard manner. An Amp/Chl LB plate was divided into 6 quadrants to accommodate up to 6 different positive clones, and care was taken to avoid the mixing of different competent cell aliquots on the plate. The plate was then incubated overnight as described above in the standard conditions.

After 14 hr., 6 sterile 8.5 mL capped 13 mm glass test tubes were prepared for mini-cultures of the transformed *E. coli*. 10 mL of LB media was brought up to an ampicillin concentration of 100 µg/mL and chloramphenicol of 25 µg/mL. 1 mL aliquots of the media was then added to 5 culture tubes and 2 mL of was added to the last culture tube. Around 10 colonies per clone was picked from the transformation plate using an inoculating loop with proper sterile technique and then dipped into the respective labeled culture tube. One of the clones was randomly chosen to inoculate into the culture tube containing 2 mL LB media as a control. The inoculated bacterial cultures were grown at 37°C in a shaking incubator at 200 rpm. After 45 min. of bacterial growth, at which the culture tubes started to appear slightly cloudy, 1 mL of the control tube was separated into a clean empty tube as the uninduced control. Isopropyl β-D-1-thiogalactopyranoside (IPTG) was added to the final concentration of 0.4 mM to all other 6 culture tubes (excluding the control tube) and grown for an additional 3 hr. to induce protein production.

The induced bacterial cultures were then transferred to clean 1.5 mL eppendorf tubes and centrifuged in a Beckman Coulter Microfuge 18 at 14,000 rpm (14,539 x g) for 5 min. to harvest the cells. The supernatant was discarded and 100-300 µL of 1x SDS-sample buffer was added to the pellet according to pellet size. The bacterial pellets were then sonicated and heated at 80°C for 5 min to extract the total proteins and break up the bacterial genomic DNA. SDS-PAGE and western blot were then run to determine the level of the expression of the TnT or

TnT fragment, with the uninduced control included to help identification of the target protein in the SDS-PAGE gel and western blot. A clone with the best protein expression would later be used for minipreparation of plasmid DNA for sequencing confirmation of the expression plasmid construct.

Plasmid Minipreparation

After the best clone was determined by miniexpression, the corresponding JM109 smear culture identified by the colony PCR screening was used to inoculate in a 50 mL tube with 5 mL of LB media brought up to a final ampicillin concentration of 100 µg/mL. The culture was inoculated using an inoculating loop by lightly touching a colony from the smear and dipping into the media. The bacterial culture was then incubated for 12 hr. at 37°C in a shaking incubator at 200 rpm. After incubation, the 50 mL tube was spun down in a Beckman GS-6R centrifuge with a GH-3.8 rotor at 3,000 rpm (1,459 x g) for 15 min. The supernatant was discarded and the tube was inverted on a paper towel to get rid of any excess supernatant. The plasmid DNA from the pellet was then purified using the GenElute™ Plasmid Miniprep Kit (Sigma) according to the manufacturer's instructions. Briefly, the pellet was suspended in RNase A solution, lysed in an SDS-alkali solution, and neutralized with binding solution. The mixture was spun to remove cell debris, proteins, lipids, SDS, and chromosomal DNA, which all appear in a viscous precipitate. The supernatant was then added to a silica spin column to absorb the plasmid DNA, followed by elution with TE buffer. The purified DNA is then analyzed using agarose gel electrophoresis to confirm the presence of the target plasmid and is then sent for DNA sequencing at a commercial service facility (GENEWIZ).

DNA Sequence Analysis

To confirm the identity of the plasmid containing the target insert, an aliquot of the purified plasmid was sent to GENEWIZ for sequencing, using the T7 forward primer and T7

terminator reverse primer that flank the cDNA insert cloned into the pET or pAED4 plasmids. The chromatograph trace generated from DNA sequencing via capillary electrophoresis was checked to ensure the sequence was clean with minimal background noise, indicating high plasmid quality. Any miscalled nucleotides and dye blots in the trace was corrected before finalizing the DNA sequence. The coding sequence was then translated into the amino acid sequence using DNASTAR Lasergene and the amino acid sequence was compared to the reference sequence in the database to confirm a 100% match.

Large Scale Protein Expression and Purification

Large Scale Expression of Recombinant Troponin T and Fragments

BL21(DE3)pLysS cells were transformed in the afternoon with recombinant plasmid containing the cDNA of interest on two 100-mm Amp/Chl plates and incubated at 37°C overnight. In the next morning, Amp and Chl was added to 8 flasks of 1 L previously prepared autoclaved LB media, to the final concentrations of 100 µg/mL and 12.5 µg/mL respectively. A 2 mL aliquot of the LB media was used as blank for spectrometry measurements of bacterial growth. A 20 mL aliquot of the LB media was transferred to a 50 mL sterile culture tube. The BL21(DE3)pLysS cells were scraped off the LB plate with a glass spreader and suspended in the 20 mL aliquot of LB. The bacterial cell suspension was pipetted up and down to ensure homogeneity and then distributed evenly to each flask. The flasks were then incubated in a 37°C incubator and shaken at 200 rpm. Bacterial growth in the culture flask was monitored by measuring OD₆₀₀. When the OD₆₀₀ reached 0.3, a 1 mL aliquot from one of the bacterial culture flasks was taken and the cells were spun down in a Beckman Coulter Microfuge 18 at 14,000 rpm (14,539 x g) to serve as an uninduced control. The bacterial cultures were then induced by adding IPTG to a final concentration of 0.4 mM. The cultures were shaken at 37°C for an additional 3 hr. for the induction of protein expression. After the protein induction phase, OD₆₀₀

measurements of the cultures were recorded and 1 mL samples of bacterial cultures were taken for collecting cells and evaluating the protein expression using SDS-PAGE and western blot.

The bacterial cultures were transferred to 1 L centrifuge bottles and centrifuged at 8,000 rpm (12,228 x g) for 15 min in a Beckman Coulter Avanti J-20 XPI using a JLA 8.1 rotor. After centrifugation, the supernatant was discarded. The bacterial pellets were put on ice, combined together and suspended in lysis buffer (50 mM, 5 mM EDTA pH 8.0), supplemented with 0.5 mM phenylmethylsulfonyl fluoride (PMSF) and 15 mM β -mercaptoethanol to a final volume of 100 mL. The bacterial cell suspension was then lysed using a French press at >500 psi for 3 passes. The lysate solution was then centrifuged at 12,000 rpm (13,845 x g) in a JA-14 rotor for 30 min to remove cell debris. 0.1 mL of the supernatant was kept for SDS-PAGE and western blot analysis of total protein expression.

Ammonium-Sulfate Precipitation

Ammonium sulfate precipitation is used for the fractionation of proteins by altering protein solubility through changes in ionic strength. Ammonium sulfate was added to the protein solution with step wise increments in concentration and the precipitate fractions were collected separately. The amount of $(\text{NH}_4)_2\text{SO}_4$ needed to bring up the protein solution to the desired saturation level at 0°C was calculated according to standard technical manuals. The protein solution was kept on ice and stirred while slowly adding the desired amount of solid $(\text{NH}_4)_2\text{SO}_4$. After adding $(\text{NH}_4)_2\text{SO}_4$, the solution was stirred on ice for 20 min. to reach equilibrium. The solution was then centrifuged at 12,000 rpm (13,845 x g) in a JA-14 rotor for 30 min. The supernatant was separated and a sample of the supernatant and pellet was taken for dialysis and SDS-PAGE/western blot analysis to evaluate the enrichment of the recombinant TnT protein. The supernatant was measured for actual volume, subsequently brought up to a higher saturation of $(\text{NH}_4)_2\text{SO}_4$ and the previous steps were repeated to separate the next

supernatant and pellet. Although the optimum $(\text{NH}_4)_2\text{SO}_4$ steps were later determined and fine-tuned experimentally, initial steps were collecting pellet of 0-20%, 20-40% and 60-80% in a new protein purification protocol. The precipitate and supernatant fractions were dialyzed overnight with three changes. The next day, SDS-PAGE and Western blot results were evaluated and the fraction containing the protein of interest was loaded into the column for further purification.

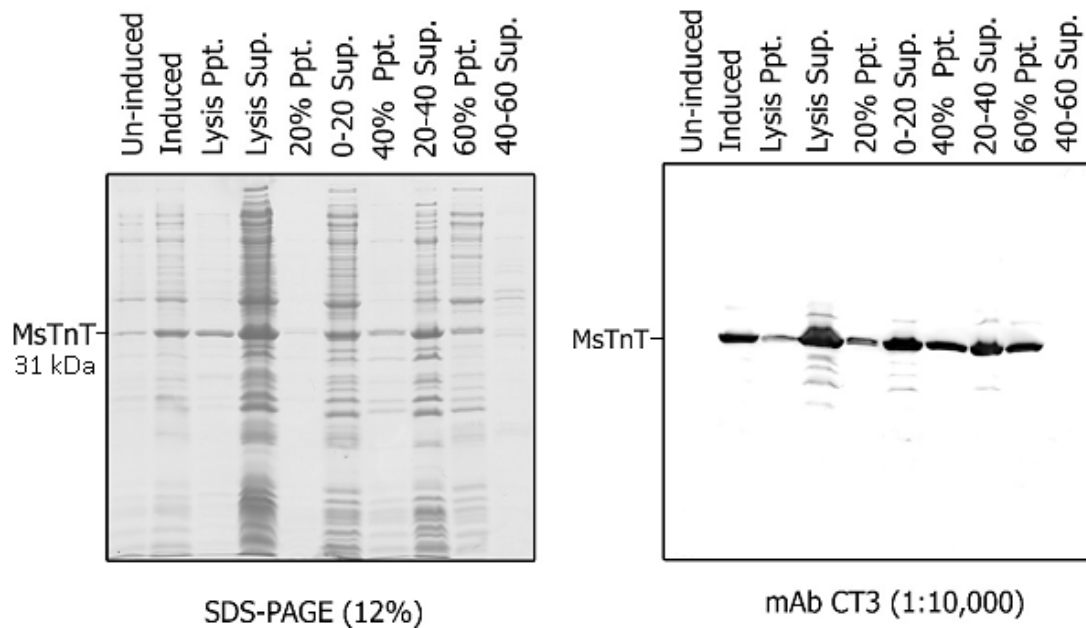


Figure 16 – SDS-PAGE and Western blot of the expression of MsTnT

Dialysis

For dialysis of protein samples, Fisherbrand regenerated cellulose dialysis tubing with a molecular weight cut off (MWCO) of 6,000-8,000 daltons was used. In order to dialysis ammonium sulfate precipitation fractions, the pellets were dissolved in a minimum amount of dialysis buffer (cold ddH₂O with 0.1 mM EDTA and 0.1% formic acid). The solution was then transferred into the dialysis tubing and the ends were clamped. The dialysis bags were then put into a container of dialysis buffer to ensure a volume ratio of 100:1 or larger of the buffer to the dialysis tubing volume. The dialysis container was kept stirring in 4°C for 4 hours or longer

between changes to ensure equilibrium between the dialysis tubing and the dialysis container.

The supernatant samples were dialyzed directly

Column Chromatography

Anion Exchange Chromatography

This technique separates proteins based on varying charge of proteins, in which protein solution (the liquid phase) is passed through a covalently cross-linked ion-agarose beads matrix (the solid phase). In the present study, the solid phase is comprised of positively charged diethylaminoethyl cellulose (DE52) beads. In order for the target protein to bind to the beads, the proteins must be negatively charged. This requires the pH of the column to be at least 1 unit higher than the PI of the target protein. Elution of proteins bound to the column is achieved by increasing ionic strength through an increasing gradient of KCl. The more tightly bound proteins elute out towards the end of the gradient, where a higher ionic strength is required to disrupt its interactions with the column beads.

A 50 mL DE52 column was first regenerated using a BioLogic LP system with the following steps:

- | | | |
|----|--------------------------------------|--|
| 1. | 1 M KCl | 20 mL |
| 2. | ddH ₂ O | 50 mL |
| 3. | 1 M HCl | 20 mL |
| 4. | 1 M NaOH | 20 mL |
| 5. | ddH ₂ O | Until pH 7 |
| 6. | 1 M Buffer A (pH depends on protein) | Until target pH reached (~10 mL) |
| 7. | Buffer A | Until target pH and conductivity reached |

Buffer A: With or without 6 M urea (for insoluble/soluble proteins), 10 mM Tris-HCl pH adjusted to target protein of interest. **Buffer B:** DE52: Buffer A + 300 mM KCl (adjust pH) .

Steps 6 and 7 were used to equilibrate the column beads to the desired pH for the run to ensure optimum separation of the target protein. The protein solution was brought up to 6 M urea in the cases of insoluble proteins in Buffer A supplemented with 0.5 mM PMSF, 0.1 mM EDTA (for inhibition of any proteases). The protein solution was centrifuged using a JA-14 rotor at 12,000 rpm for 30 minutes. 15 mM β -Mercaptoethanol was added to the protein sample and 6 mM β -Mercaptoethanol was added to the column buffers. The protein solution was then loaded into the column and the following program was run through the BioLogic LP system at a flow of 1 mL/min for all steps:

1	Buffer C	100 min (Assuming sample size is 100 mL)
2.	Buffer A	50 min
3.	Buffer B	300 min
4.	Buffer B 0-100%	50 min
	Fraction collection	6 min per fraction, collect 56 min to 530 min

The outflow of the column was monitored using an in line UV monitor for absorbance at 280 nm. SDS-PAGE and western blots were run for the protein containing fractions to evaluate the peak fraction containing the target protein. Those fractions were then dialyzed and lyophilized. An example of the DE52 column profile is shown in Figure 17.

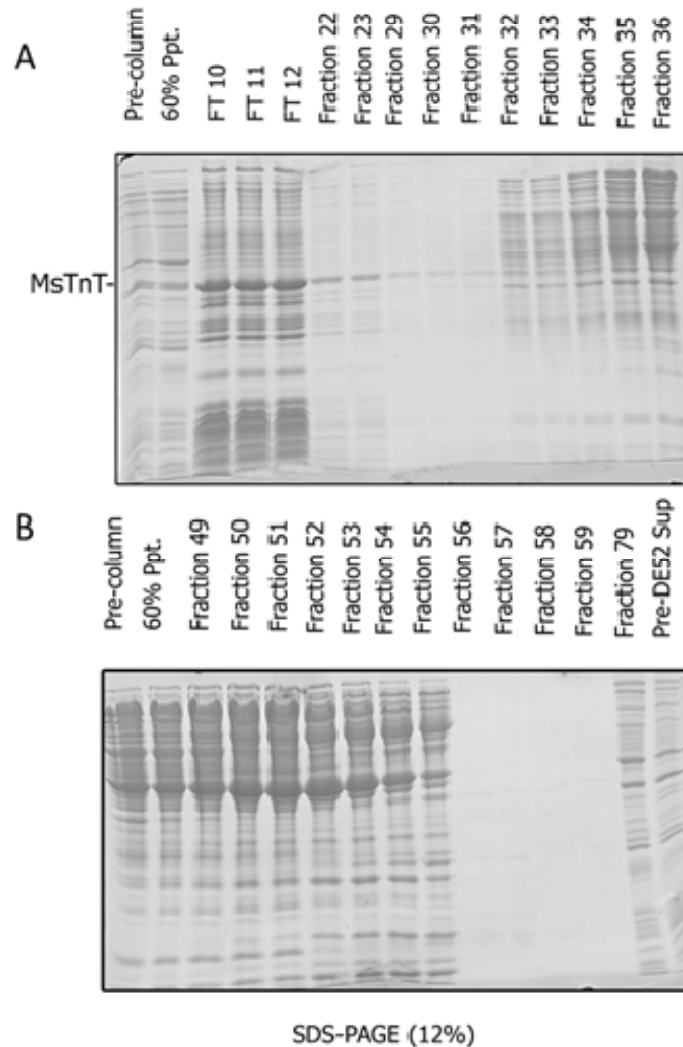


Figure 17 – DE52 anion exchange column purification of MsTnT. (A): MsTnT starts to elute at fraction 22 and ends at fraction 31. (B): Higher molecular weight contaminant proteins eluting at higher concentrations of KCl

Size-exclusion Chromatography

In order to further separate impure protein fractions by size, a 2.5 x 120 cm (588 mL) G75 gel filtration column was used. The G75 column was first washed using a BioLogic LP system with one column volume equivalent of the buffer containing 6 M urea, 0.5 M KCl, 10 mM imidazole, 0.1 mM EDTA, pH 7.0, and supplemented with 6 mM β -mercaptoethanol (“G75 buffer”) at a flow rate of 0.5 mL/min. The lyophilized protein to be loaded into the column was dissolved in a minimum volume of G75 buffer (<5 mL when possible). The

protein sample solution was centrifuged in a Beckman Coulter Microfuge 18 at 12,000 RPM (10,682 x g) for 5 minutes and loaded onto the G75 column. The following program was run with BioLogic LP system:

Flow rate set to **0.5 mL/min**

1. G75 Buffer 1280 min

Fraction collection 12-16 min per fraction, collect 200 to 1280 min

The column fractions were monitored using a UV monitor at 280 nm. SDS-PAGE and Western blot of the fractions were run to evaluate which fraction contained the target protein at the highest amount and purity. Those fractions were then dialyzed and lyophilized.

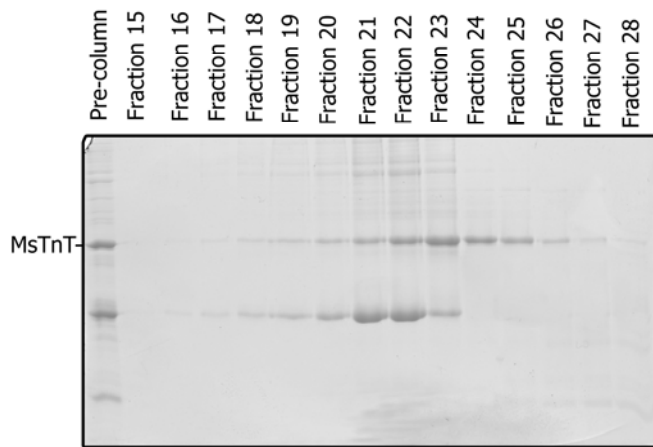


Figure 18 – G75 Size exclusion column purification of MsTnT. Pure fractions of MsTnT starts to elute at fraction 24 and ends at fraction 27

Metal Ion Affinity Chromatography

High efficiency metal ion affinity chromatography was used to purify TnT fragments that expressed in *E. coli* only at very low levels. cDNAs encoding the TnT fragments were cloned into a modified plasmid vector encoding an N-terminal affinity tag, Tx3 (HEEAHHEEAHHEEAH), to facilitate the purification via metal ion affinity chromatography. This repeating Tx sequence is a metal binding cluster that has been naturally found in fTnT in chicken breast muscle, which indicates that this sequence is well tolerated in TnT (Jin &

Smillie, 1994). The use of Tx sequence as an affinity purification tag allows for highly effective purification of the target protein using a Zn(II) column in high stringency buffer conditions (e.g., 6 M urea, 1 M KCl), which demonstrate the greater effectiveness of Tx3 tag over the commonly used polyhistidine tags (Jin & Lin, 1988; Arnold & Haymore, 1991; Ogut & Jin, 1996; Jin et al., 2000).

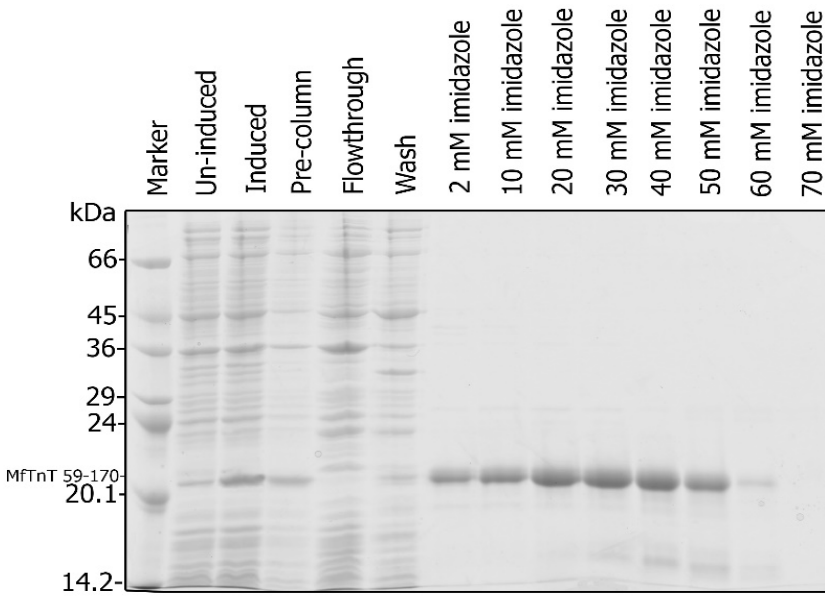
The column used for this procedure was a 20 mL column containing Chelating Sepharose Fast Flow beads (GE Healthcare). The column was first regenerated and charged with Zn²⁺ in the following manner:

1.	10 mM EDTA in 1 M KCl	20 mL
2.	ddH ₂ O	50 mL
3.	0.1M NaOAc (pH 4.0)	20 mL
4.	0.1M ZnCl ₂ in 0.1 NaoAc (pH 4)	20 mL
5.	0.1M NaOAc (pH 4.0)	20 mL
6.	ddH ₂ O	20 mL
7.	0.1 M phosphate buffer (pH 7.4)	20 mL
8.	Lysis buffer (pH 7.4)	20 mL

During this procedure, competent cells were transformed and protein was expressed as described above. After centrifuging the bacterial cultures, the bacterial pellets were combined and suspended in a urea lysis buffer (6 M urea, 1 M KCl and 20 mM phosphate buffer, pH 7.4) or non-urea low salt lysis buffer (30 mM KCl, 20 mM phosphate buffer, pH 7.4). In the present study, only Tx3-McTnT T1 required the use of the non-urea lysis buffer as it had weaker binding in the urea lysis buffer.

After suspending the bacterial pellet in lysis buffer and lysis of cells using French press

as above, the lysate was centrifuged using a JA-14 at 12,000 RPM (13,845 x g) for 30 min. and the supernatant was loaded into an equilibrated Zn^{2+} column. After the flowthrough was collected, the column was washed with 100 mL of lysis buffer. The column was then eluted with 1 column volume each step of increasing concentrations of imidazole (10 mM to 100 mM) to elute the metal-binding recombinant TnT fragment. The peak fractions were identified with SDS-PAGE and Western blot, dialyzed, and lyophilized.



SDS-PAGE 12% (29:1)

Figure 19 – SDS-PAGE and Western blot of Zn^{2+} affinity column purification of Tx3-MfTnT middle fragment. Pure fractions of the fragment elute from 2 mM to 60 mM imidazole with bacterial protein contaminants eluting during the flowthrough and washing step.

Lyophilization of Protein Samples

Protein samples were lyophilized using a Labconco FreeZone 4.5 Liter system. After fully dialyzed, the protein solutions were frozen in a dry ice box for 45 min while positioned to achieve a large surface area. The flasks were then quickly connected to the drying chamber of the lyophilizer for freeze-drying.

Tropomyosin Binding Assay

Solid-Phase Microplate Protein-Binding Assay

The tropomyosin binding assay used in the present study is an ELISA-based solid-phase

microplate protein-binding assay which takes advantage of immunological detection in a high throughput plate form to assess the tropomyosin binding affinities of different TnT constructs (Biesiadecki & Jin, 2011).

TnT was coated and immobilized non-covalently on a polystyrene microtiter plate while the binding partner applied to TnT was rabbit α/β skeletal muscle tropomyosin previously prepared in Dr. Jin's laboratory (Smillie, 1982). The primary antibody applied to detect the bound tropomyosin was a monoclonal antibody against both of the muscle Tm isoforms (Lin, Chou, & Lin, 1985). The binding of Tm to different TnT constructs was elucidated by the binding of Tm at a series of concentrations and different amounts of Tm left binding to TnT after stringent washes. The difference in Tm binding is quantitatively determined by colorimetric reaction via the use of Horseradish peroxidase (HRP)-labeled second antibody. Thus, this assay gives information regarding binding affinity and binding strength between the two proteins, Tm and TnT.

The purified TnT proteins were dissolved in Buffer A (100 mM KCl, 1 mM ethylene glycol tetraacetic acid (EGTA), 3 mM MgCl₂, 20 mM piperazine-N,N'-bis(2-ethanesulfonic acid) (PIPES), pH 7.0) at 5 μ g/mL to coat 96-well polystyrene microtiter plates at 100 μ L/well at 4°C overnight. Free TnT proteins were removed by washing with Buffer T (Buffer A plus 0.05% Tween 20) for three times over a 10 min. period. The plate was then blocked with Buffer T + 1% BSA at room temperature for 1 hr. Serial dilutions of rabbit α/β skeletal muscle tropomyosin in Buffer T containing 0.1% BSA were added to the plate at 100 μ L/well and incubated at room temperature for 2 hr. The plates were washed three times with Buffer T and an anti-Tm mAb CH1 (1:10,000) was added to the plate at 100 μ L/well and incubated at room temperature for 1 hr. After three Buffer T washes, goat anti-mouse HRP-labeled second antibody (1:4,500) was added to the plate at 100 μ L/well and incubated at room temperature for

45 min. After three Buffer T washes, the amount of Tm bound to the immobilized TnT in each well was quantified using H₂O₂-ABTS (2,20-azinobis(3-ethylbenzthiazoline-6-sulfonic acid) substrate reaction catalyzed by HRP. The A_{415nm} values in the linear course of the color development were monitored for each assay well against the reference wavelength of 655 nm using a Bio-Rad Benchmark automated microplate reader and recorded to construct Tm-binding curves for each set of TnT proteins. The experiments were done in triplicate wells and repeated.

Statistical Analysis

The raw absorbance values of each binding curve were compared via repeated measures using two-way ANOVA using GraphPad Prism software. The column means were compared across raw data binding curves and a Tukey's multiple comparisons test was conducted with a 0.05 significance level.

In order to obtain 50% maximum binding values, sigmoidal dose-response (variable slope) curves were fitted to each binding curve with the least squares fitting method.

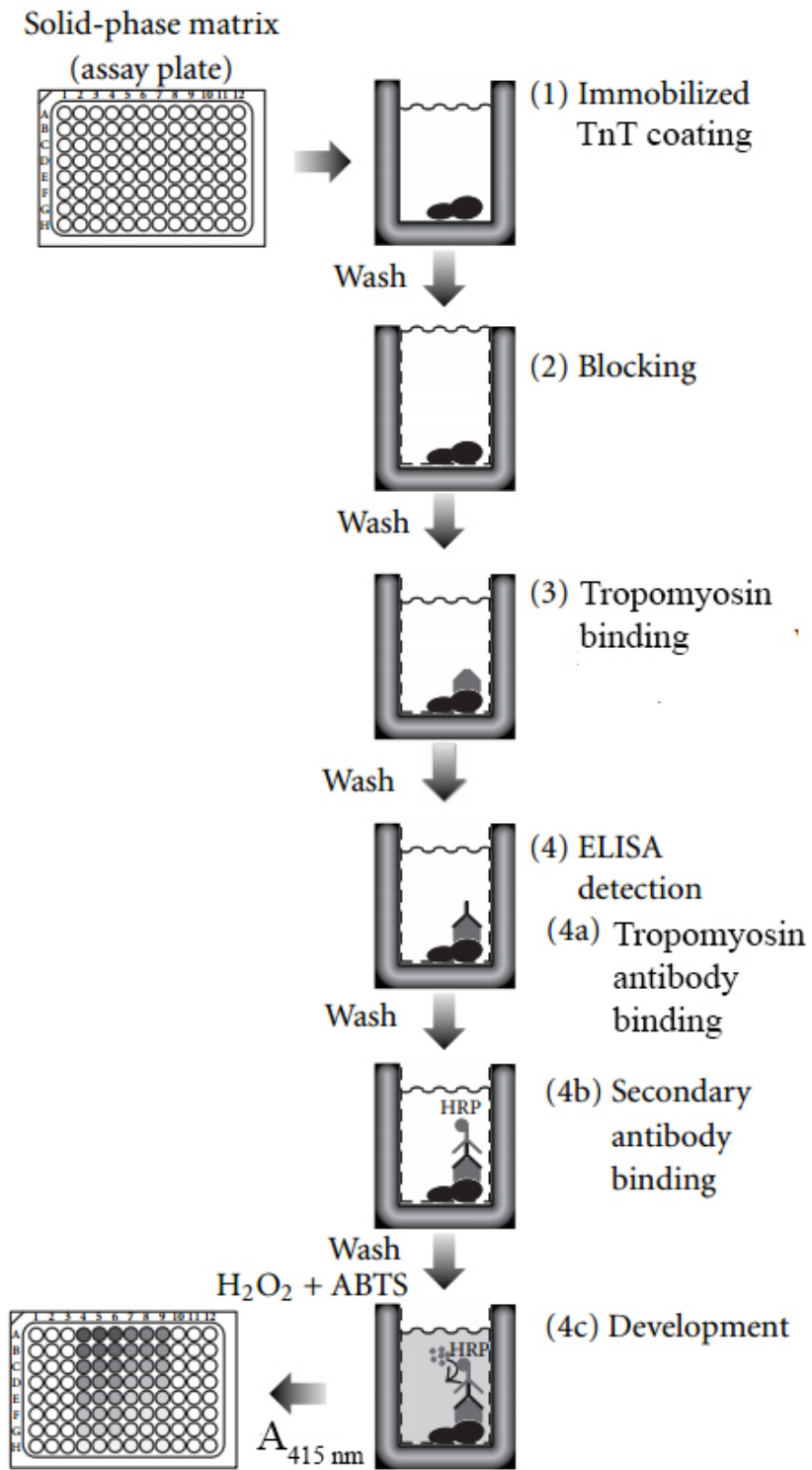


Figure 20 - ELISA-based solid-phase protein binding assay

CHAPTER 3

RESULTS

Tropomyosin Binding Affinity of T2 Fragments of Different TnT Isoforms

There was no significant difference in Tm binding affinity among the muscle fiber-specific T2 fragments. These fragments are comprised of their respective T2 binding regions, which have the site 2 Tm binding site.

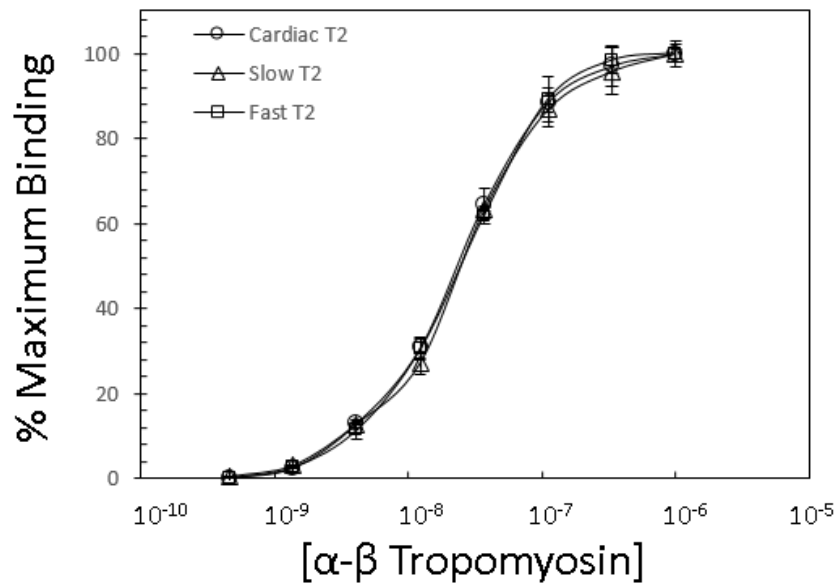


Figure 21 – No significant differences in Tm binding affinity between T2 fragments across isoforms. (P=0.8480 for cardiac T2 vs. slow T2, P=0.9895 for fast T2 vs. slow T2 by Fisher test in Two Way ANOVA).

Tropomyosin Binding Affinity of T1 Fragments of Different TnT Isoforms

There was a significant difference in Tm binding affinity among the T1 fragments of different muscle fiber-specific isoforms, with fast T1 having the highest Tm binding affinity, then cardiac and lastly slow T1 with the lowest Tm binding affinity. These fragments are comprised of their respective N-terminal hypervariable regions and middle conserved regions, which contain the Tm binding site 1.

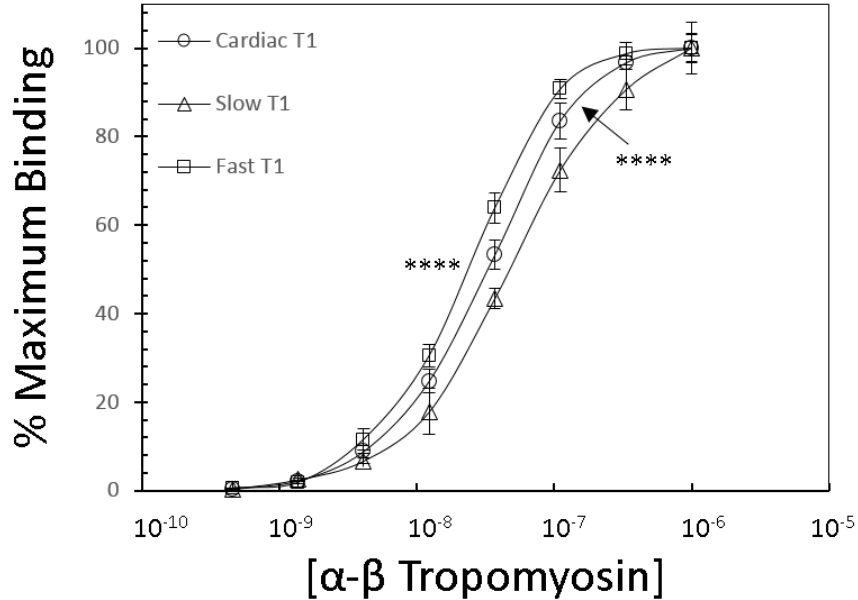


Figure 22 – Significant differences in Tm binding affinity between T1 fragments across isoforms. (****P < 0.0001 for cardiac T1 vs. slow T1, ****P < 0.0001 for fast T1 vs. slow T1 by Fisher test in Two Way ANOVA)

Tropomyosin Binding Affinity of Middle Fragments of Different TnT Isoforms

There was no significant difference in Tm binding affinity between the middle fragments among different muscle-fiber specific isoforms. These fragments are comprised of their conserved middle regions, which lack their respective N-terminal hypervariable regions but retain the site 1 Tm binding site.

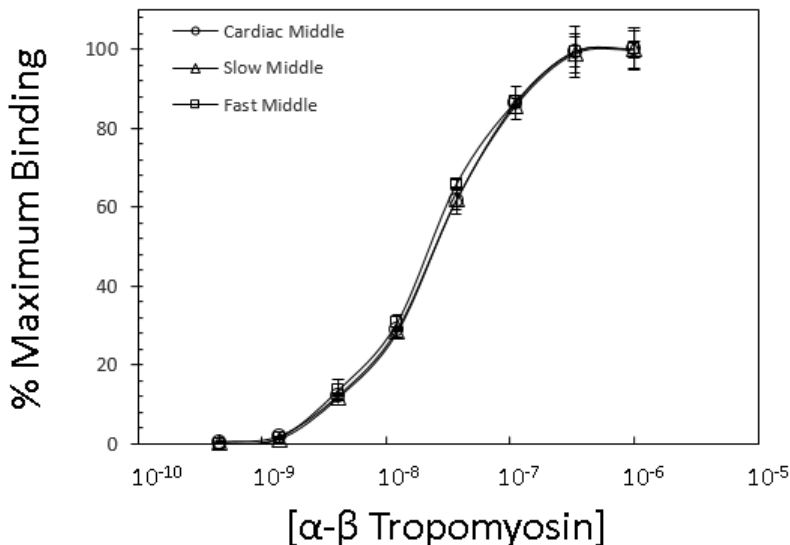


Figure 23 - No significant differences in Tm binding affinity between middle fragments across isoforms. (P=0.9814 for cardiac middle vs. slow middle, P=0.0538 for fast middle vs. slow middle by Fisher test in Two Way ANOVA)

Tropomyosin Binding Affinity of Intact TnT Isoforms

There was a significant difference in T_m binding affinity among the intact TnTs of different muscle fiber-specific isoforms, with fast TnT having the highest T_m binding affinity, then cardiac and lastly slow TnT with the lowest T_m binding affinity. These TnTs are comprised of their respective T1 and T2 regions which each contain T_m binding sites 1 and 2, respectively.

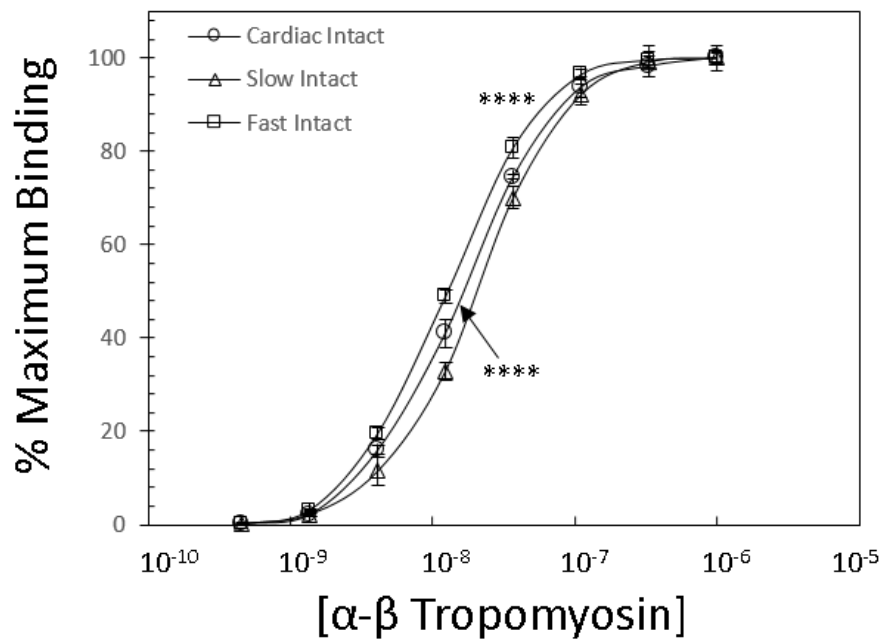
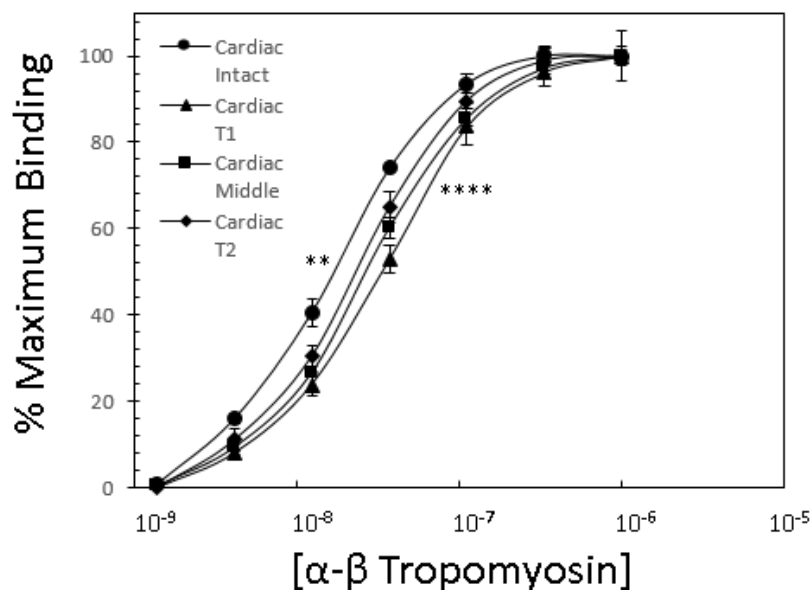


Figure 24 - Significant differences in T_m binding affinity between intact TnT isoforms. (**** $P < 0.0001$ for cardiac intact vs. slow intact, **** $P < 0.0001$ for fast intact vs. slow intact by Fisher test in Two Way ANOVA)

Tropomyosin Binding Affinity of TnT Comparison within Species and Isoform

Intact cardiac TnT had the highest T_m binding affinity, followed by the cardiac middle and T2 fragments, which contain the T_m binding site 1 and 2, respectively (these two did not have significantly different T_m binding). The cardiac T1 fragment had the lowest T_m binding affinity, and contained its respective N-terminal hypervariable region and site 1 T_m binding site.

Figure 25 - Comparison of Tm binding affinity of intact, T1, T2 and middle fragments of cardiac TnT. There were significant differences in Tm binding affinity between T2, T1 and intact, with no significant difference between middle and T2; all TnTs are within the same species and isoform. (**P < 0.0026 for cardiac intact vs. cardiac T2, ****P < 0.0001 for cardiac T1 vs. cardiac T2, and P=0.4978 for cardiac middle vs. T2 by Fisher test in Two Way ANOVA)



Below is a summary of each set of ELISA experiments. In the Table, Tm binding refers to the qualitative difference of Tm binding, where Ref is the reference curve used for comparison, and + and - represent an increase and decrease in Tm binding, respectively. EC50 values are the Tm concentrations to reach 50% maximum Tm binding for each TnT construct.

Table 2 – Summary of Protein Binding Experiments

TnT Fragment	Cardiac T2	Slow T2	Fast T2	
Tm Binding	=	Ref	=	
EC50	2.279E-08	2.443E-08	2.545E-08	
Std. Dev.	0.01687	0.01546	0.01593	
TnT Fragment	Cardiac T1	Slow T1	Fast T1	
Tm Binding	+	Ref	++	
EC50	3.338E-08	5.103E-08	2.491E-08	
Std. Dev.	0.02425	0.03049	0.03195	
TnT Fragment	Cardiac Middle	Slow Middle	Fast Middle	
Tm Binding	=	Ref	=	
EC50	2.481E-08	2.744E-08	2.301E-08	
Std. Dev.	0.01482	0.01392	0.01428	
TnT Fragment	Cardiac Intact	Slow Intact	Fast Intact	
Tm Binding	+	Ref	++	
EC50	1.606E-08	2.007E-08	1.283E-08	
Std. Dev.	0.009816	0.01101	0.009500	
TnT/TnT Fragment	Cardiac Intact	Cardiac T1	Cardiac Middle	Cardiac T2
Tm Binding	+	-	=	Ref
EC50	1.630E-08	3.213E-08	2.707E-08	2.270E-08
Std. Dev.	0.01243	0.01825	0.01350	0.01721

CHAPTER 4

DISCUSSION

Methodology and Rationale

This is the first study that has compared intact TnTs and TnT fragments in order to elucidate the differences in intrinsic site 1 and site 2 Tm binding affinity across muscle fiber-specific isoforms. Previous studies that investigated TnT's Tm binding affinity have relied on enzymatic and chemical cleavage of intact TnT to generate various fragments that contain or lack specific TnT Tm binding sites (Mak & Smillie, 1981; Nakamura, Yamamoto, Hashimoto, & Ohtsuki, 1981; Pearlstone & Smillie, 1982; Heeley et al., 1987; Jin et al., 2000). In this study, molecular biology techniques were used to generate intact TnT and TnT fragments that allowed comparison and elucidation of the structure and function of TnT beyond the conventional comparison of the T1 and T2 regions of TnT. These two regions produced by enzymatic or chemical cleavage have been useful to investigate the Tm binding affinity of T1 and T2 regions. However, this approach was not particularly useful to understand the intrinsic Tm binding affinity of site 1 which was further explored in this study. The expression and purification of TnT fragments with the aid of affinity tag chromatography has allowed further investigation into the role of TnT's Tm binding sites and the role of the N-terminal hypervariable region in the modulation of TnT-Tm binding

The Role of TnT's N-Terminal Hypervariable Region in Muscle Fiber-Specific Isoforms

One of the main findings in this study is that TnT's N-terminal hypervariable region is responsible for the significant differences in tropomyosin binding across muscle-fiber specific isoforms.

When the T1 fragments among different muscle fiber-specific isoforms are compared, there is a significant difference in Tm binding (Figure 22). Among the T1 fragments across

isoforms, fast TnT was observed to have the highest binding affinity to Tm, followed by cardiac and then slow. This pattern was also observed in the intact TnT, with significant differences across intact TnT isoforms (Figure 24). Since the T1 fragments only contain their respective N-terminal hypervariable region in addition to the highly conserved middle Tm binding site 1, the presence of this N-terminal hypervariable region is responsible for variably modulating site 1's Tm binding affinity across isoforms, both in intact TnTs and TnT T1 fragments of muscle fiber-specific isoforms.

It is important to note that this significant differences in Tm binding affinity in intact TnTs is not decreased with the presence of both Tm binding sites despite this study's observation that there is no significant difference in site 2's binding affinity across isoforms (Figure 21). The observation that the significant differences in intact TnT isoforms are still present despite the similar Tm binding affinity of site 2 across muscle specific isoforms indicate that the differences in TnT isoforms arise because of the modulation site 1's Tm binding affinity by the N-terminal hypervariable region.

When the N-terminal hypervariable region is removed and only the middle region of TnT is compared across isoforms, the significant difference in site 1 Tm binding affinity is abolished (Figure 23). This indicates that the difference in site 1's Tm binding affinity among the T1 fragments across isoforms is due to the presence of the N-terminal hypervariable region. This observation is consistent with previous data showing that the N-terminal hypervariable region not only alters TnT's overall conformation, but most likely modulates the more proximal central Tm-binding site as opposed to the more distal TnT binding site (J. Wang & Jin, 1998; Jin et al., 2000).

Additionally, this study also corroborated previous observations that the N-terminal truncation of cTnT results in an overall increase in intact TnT's binding affinity to Tm (Fisher et

al., 1995; Feng et al., 2008). The mechanism of this phenomenon is more apparent in this study, where it was shown that the cTnT middle fragment exhibited a higher T_m binding affinity than the T1 fragment (Figure 25). This indicates that the N-terminal truncation of intact cardiac TnT results in an overall increase of T_m binding largely due to the lack of modulation of site 1's T_m binding affinity by the N-terminal hypervariable region.

T_m Binding Affinity of Sites 1 and 2

This study also evaluated the T_m binding affinity of each site across isoforms as well as within a specific isoform and species. T2 fragments had an overall higher T_m binding affinity compared to the T1 fragments (Figure 25). This is in line with previous observations decades ago showing that the fTnT T2 has the greater T_m binding affinity compared to fTnT T1 when both proteins are analyzed on an α -tropomyosin binding column (Heeley et al., 1987).

Although this study used α - β tropomyosin in the binding assays, previous studies have shown that the TnT fragments do not each have their own "specific preference" in regards to T_m binding affinity. Instead, it was observed that TnT fragments and intact TnT all exhibit a higher binding affinity to α -tropomyosin and a lower binding β -tropomyosin. Because of this observation, the conclusions reached in this study regarding T_m binding affinity of TnT fragments would most likely hold if α -tropomyosin or β -tropomyosin was used (Heeley et al., 1987).

In the experiment comparing intact TnT and TnT fragments within the same isoform and species, the middle cTnT fragment's binding affinity was not significantly different compared to cTnT T2. This indicates that without the modulatory effect of the N-terminal hypervariable region, the intrinsic T_m binding affinity of site 1 is not significantly different to site 2's T_m binding affinity, and that T_m binding affinity of both sites is high (Figure 25). This is demonstrated by the observation that the T2 fragments across isoforms exhibit no significant

differences in binding affinity to tropomyosin while the T1 fragments across isoforms exhibit significant differences in binding affinity to tropomyosin due to their respective N-terminal hypervariable region.

Conclusions

This study demonstrated that N-terminal variable region is a regulatory structure for functional alteration of TnT muscle fiber-specific isoforms. In the absence of the N-terminal variable region of TnT, TnT's conserved site 1 and site 2 tropomyosin binding sites across isoforms do not have any significant difference in Tm binding affinity (Figure 25). This indicates that the N-terminal hypervariable region is largely responsible for the functional difference of TnT across isoforms by variably modulating the Tm binding affinity of site 1. A discrepancy in past literature (Pearlstone & Smillie, 1982; Heeley et al., 1987; Jin & Chong, 2010) showing different Tm binding of T1 fragments vs. T2 Tm binding is explained by the data in this study by demonstrating that site 1's Tm binding affinity is differentially modulated by the N-terminal hypervariable region across isoforms (Figure 26).

This difference in modulation of site 1 and possibly site 2 is largely responsible for altering the overall conformation of TnT and thus conformation of the troponin complex (Figure 26), which subsequently modulates the calcium activated regulation of striated muscle contraction (Ebashi & Endo, 1968; Meinrenken, 1969; Gazith et al., 1970; Spudich & Watt, 1971; Mihashi, 1972; Vaneerd & Kawasaki, 1973; Rupp, 1983; Biesiadecki et al., 2007; Sheng & Jin, 2014), and thus plays a role in the functional difference of muscle fiber type-specific, developmental, splice variant, and pathogenic TnT isoforms.

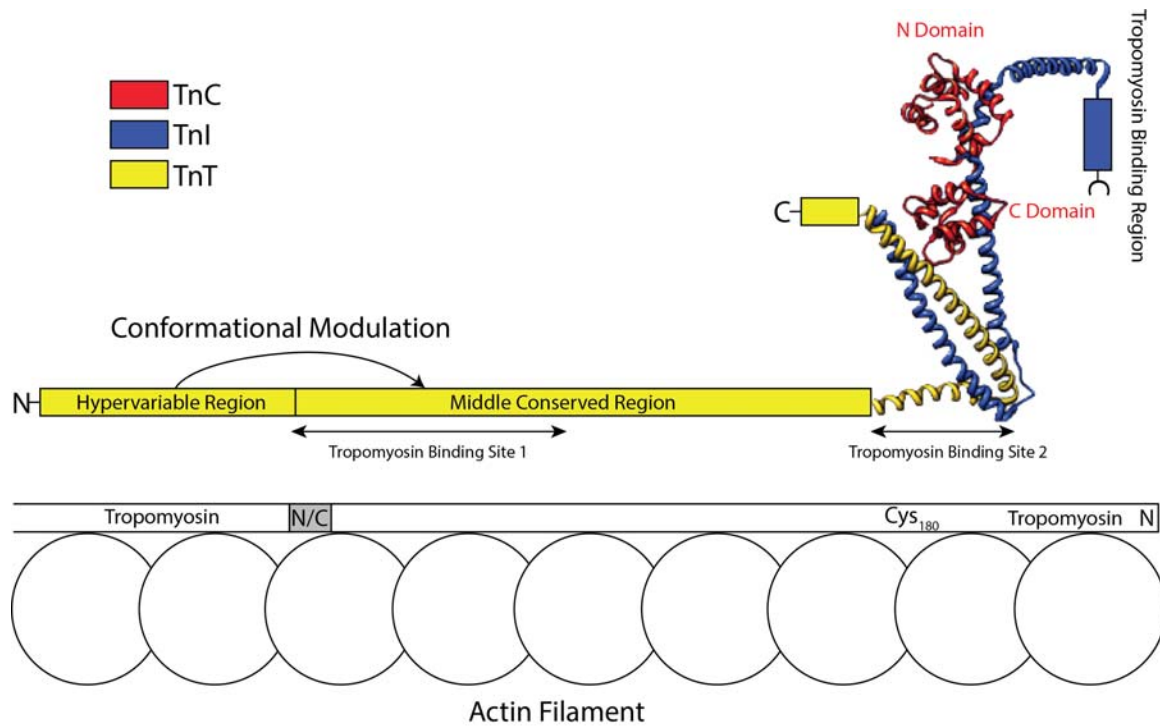


Figure 26 – A model summarizing the findings. The N-terminal hypervariable region modulates the Tm binding affinity of Tropomyosin Binding Site 1 and thus results in variable Tm binding affinity of Site 1 across TnT muscle fiber specific isoforms. The partial high resolution structure of the Troponin complex was redrawn from previously published crystallography data (Takeda et al., 2003; Vinogradova et al., 2005; Sheng & Jin, 2014)

REFERENCES

1. Akella, A. B., Ding, X. L., Cheng, R., & Gulati, J. (1995). Diminished Ca²⁺ sensitivity of skinned cardiac muscle contractility coincident with troponin T-band shifts in the diabetic rat. *Circ Res*, 76(4), 600-606.
2. Anderson, P. A., Greig, A., Mark, T. M., Malouf, N. N., Oakeley, A. E., Ungerleider, R. M., Kay, B. K. (1995). Molecular basis of human cardiac troponin T isoforms expressed in the developing, adult, and failing heart. *Circ Res*, 76(4), 681-686.
3. Arnold, F. H., & Haymore, B. L. (1991). Engineered Metal-Binding Proteins - Purification to Protein Folding. *Science*, 252(5014), 1796-1797.
4. Artimo, P., Jonnalagedda, M., Arnold, K., Baratin, D., Csardi, G., de Castro, E., Stockinger, H. (2012). ExPASy: SIB bioinformatics resource portal. *Nucleic Acids Res*, 40(Web Server issue), W597-603.
5. Biesiadecki, B. J., Chong, S. M., Nosek, T. M., & Jin, J. P. (2007). Troponin T core structure and the regulatory NH₂-terminal variable region. *Biochemistry*, 46(5), 1368-1379.
6. Biesiadecki, B. J., & Jin, J. P. (2011). A high-throughput solid-phase microplate protein-binding assay to investigate interactions between myofilament proteins. *J Biomed Biotechnol*, 2011, 421701.
7. Breitbart, R. E., & Nadalginard, B. (1986). Complete Nucleotide-Sequence of the Fast Skeletal Troponin T-Gene - Alternatively Spliced Exons Exhibit Unusual Interspecies Divergence. *J Mol Biol*, 188(3), 313-324.
8. Breitbart, R. E., & Nadalginard, B. (1987). Developmentally Induced, Muscle-Specific Trans Factors Control the Differential Splicing of Alternative and Constitutive Troponin-T Exons. *Cell*, 49(6), 793-803.

9. Breitbart, R. E., Nguyen, H. T., Medford, R. M., Destree, A. T., Mahdavi, V., & Nadalginard, B. (1985). Intricate Combinatorial Patterns of Exon Splicing Generate Multiple Regulated Troponin-T Isoforms from a Single Gene. *Cell*, *41*(1), 67-82.
10. Briggs, M. M., & Schachat, F. (1996). Physiologically regulated alternative splicing patterns of fast troponin T RNA are conserved in mammals. *American Journal of Physiology-Cell Physiology*, *270*(1), C298-C305.
11. Castillo, A., Nowak, R., Littlefield, K. P., Fowler, V. M., & Littlefield, R. S. (2009). A Nebulin Ruler Does Not Dictate Thin Filament Lengths. *Biophys J*, *96*(5), 1856-1865.
12. Chandra, M., Kim, J. J., & Solaro, R. J. (1997). N-terminal deletion of cardiac troponin T reduces force but does not alter Ca^{2+} -sensitivity or co-operativity in skinned rat cardiac fibers. *Biophys J*, *72*(2), Mp195-Mp195.
13. Chong, S. M., & Jin, J. P. (2009). To investigate protein evolution by detecting suppressed epitope structures. *J Mol Evol*, *68*(5), 448-460.
14. Cooper, T. A., & Ordahl, C. P. (1985). A Single Cardiac Troponin-T Gene Generates Embryonic and Adult Isoforms Via Developmentally Regulated Alternate Splicing. *Journal of Biological Chemistry*, *260*(20), 1140-1148.
15. Dabrowska, R., Nowak, E., Podlubnaya, Z., & Drabikowski, W. (1975). Interaction of Troponin Components with F-Actin and F-Actin-Tropomyosin Complex. *Biochim Biophys Acta*, *400*(1), 54-61.
16. Dabrowska, R., Podlubnaya, Z., Nowak, E., & Drabikowski, W. (1976). Interaction of Tropomyosin with Troponin Components. *J Biochem*, *80*(1), 89-99.
17. Dowben, R. M., Ford, C. C., & Bunting, J. R. (1976). Interaction of Tropomyosin, Troponin, and Troponin-C with Trivalent Lanthanide Ions. *Federation Proceedings*, *35*(3), 299-299.

18. Drabikow.W, & Nonomura, Y. (1968). Interaction of Troponin with F-Actin and its Abolition by Tropomyosin. *Biochim Biophys Acta*, 160(1), 129-131
19. Drabikow.W, Nowak, E., Barylko, B., & Dabrowsk.R. (1973). Troponin - Its Composition and Interaction with Tropomyosin and F-Actin. *Cold Spring Harbor Symposia on Quantitative Biology*, 37, 245-249.
20. Ebashi, S. (1963). Third Component Participating in Superprecipitation of Natural Actomyosin. *Nature*, 200(491), 1010.
21. Ebashi, S., & Ebashi, F. (1965). Alpha-Actinin a New Structural Protein from Striated Muscle .I. Preparation and Action on Actomyosin-Atp Interaction. *J Biochem*, 58(1), 7-12
22. Ebashi, S., & Endo, M. (1968). Calcium ion and muscle contraction. *Prog Biophys Mol Biol*, 18, 123-183.
23. Endo, M. (2008). Calcium ion and troponin: Professor S. Ebashi's epoch-making achievement. *Biochem Biophys Res Commun*, 369(1), 30-33.
24. Feng, H. Z., Biesiadecki, B. J., Yu, Z. B., Hossain, M. M., & Jin, J. P. (2008). Restricted N-terminal truncation of cardiac troponin T: a novel mechanism for functional adaptation to energetic crisis. *J Physiol*, 586(14), 3537-3550.
25. Feng, H. Z., Chen, G., Nan, C., Huang, X., & Jin, J. P. (2014). Abnormal splicing in the N-terminal variable region of cardiac troponin T impairs systolic function of the heart with preserved Frank-Starling compensation. *Physiol Rep*, 2(9): 1-15.
26. Fisher, D., Wang, G., & Tobacman, L. S. (1995). NH₂-terminal truncation of skeletal muscle troponin T does not alter the Ca²⁺ sensitivity of thin filament assembly. *J Biol Chem*, 270(43), 25455-25460.
27. Gahlmann, R., Troutt, A. B., Wade, R. P., Gunning, P., & Kedes, L. (1987). Alternative

- Splicing Generates Variants in Important Functional Domains of Human Slow Skeletal Troponin-T. *Journal of Biological Chemistry*, 262(33), 16122-16126.
28. Gazith, J., Himmelfarb, S., & Harrington, W. F. (1970). Studies on the subunit structure of myosin. *J Biol Chem*, 245(1), 15-22.
 29. Gimona, M., Watakabe, A., & Helfman, D. M. (1995). Specificity of Dimer Formation in Tropomyosins - Influence of Alternatively Spliced Exons on Homodimer and Heterodimer Assembly. *Proc Natl Acad Sci U S A*, 92(21), 9776-9780.
 30. Gomes, A. V., Guzman, G., Zhao, J. J., & Potter, J. D. (2002). Cardiac troponin T Isoforms affect the Ca²⁺ sensitivity and inhibition of force development - Insights into the role of troponin T isoforms in the heart. *Journal of Biological Chemistry*, 277(38), 35341-35349.
 31. Gomes, A. V., Potter, J. D., & Szczesna-Cordary, D. (2002). The role of troponins in muscle contraction. *IUBMB Life*, 54(6), 323-333.
 32. Goody, R. S. (2003). The missing link in the muscle cross-bridge cycle. *Nature Structural Biology*, 10(10), 773-775.
 33. Hall, J. E., & Guyton, A. C. (2011). *Guyton and Hall textbook of medical physiology* (12th ed.). Philadelphia, Pa.: Saunders/Elsevier.
 34. Hanson, J. (1968). Recent x-ray diffraction studies of muscle. *Q Rev Biophys*, 1(2), 177-216.
 35. Hanson, J., & Lowy, J. (1963). Structure of F-Actin and of Actin Filaments Isolated from Muscle. *J Mol Biol*, 6(1), 46-&.
 36. Heeley, D. H., Golosinska, K., & Smillie, L. B. (1987). The effects of troponin T fragments T1 and T2 on the binding of nonpolymerizable tropomyosin to F-actin in the presence and absence of troponin I and troponin C. *J Biol Chem*, 262(21), 9971-9978.

37. Herman, I. M. (1993). Actin isoforms. *Curr Opin Cell Biol*, 5(1), 48-55.
38. Holmes, K. C., Popp, D., Gebhard, W., & Kabsch, W. (1990). Atomic model of the actin filament. *Nature*, 347(6288), 44-49.
39. Horowitz, R., Kempner, E. S., Bisher, M. E., & Podolsky, R. J. (1986). A physiological role for titin and nebulin in skeletal muscle. *Nature*, 323(6084), 160-164.
40. Hoyle, G. (1969). Comparative Aspects of Muscle. *Annual Review of Physiology*, 31, 43-84.
41. Huang, Q. Q., Brozovich, F. V., & Jin, J. P. (1999). Fast skeletal muscle troponin T increases the cooperativity of transgenic mouse cardiac muscle contraction. *J Physiol*, 520 Pt 1, 231-242.
42. Huxley, A. F., & Niedergerke, R. (1954). Structural Changes in Muscle during Contraction - Interference Microscopy of Living Muscle Fibres. *Nature*, 173(4412), 971-973.
43. Huxley, H., & Hanson, J. (1954). Changes in the Cross-Striations of Muscle during Contraction and Stretch and Their Structural Interpretation. *Nature*, 173(4412), 973-976.
44. Huxley, H. E. (1990). Sliding Filaments and Molecular Motile Systems. *Journal of Biological Chemistry*, 265(15), 8347-8350.
45. Jha, P. K., Leavis, P. C., & Sarkar, S. (1996). Interaction of deletion mutants of troponins I and T: COOH-terminal truncation of troponin T abolishes troponin I binding and reduces Ca^{2+} sensitivity of the reconstituted regulatory system. *Biochemistry*, 35(51), 16573-16580.
46. Jin, J. P. (2000). Titin-thin filament interaction and potential role in muscle function. *Regulatory Mechanisms of Striated Muscle Contraction*, 481, 319-333; discussion 334-315.

47. Jin, J. P., Chen, A., Ogut, O., & Huang, Q. Q. (2000). Conformational modulation of slow skeletal muscle troponin T by an NH₂-terminal metal-binding extension. *Am J Physiol Cell Physiol*, 279(4), C1067-1077.
48. Jin, J. P., Chen, A. H., & Huang, Q. Q. (1998). Three alternatively spliced mouse slow skeletal muscle troponin T isoforms: conserved primary structure and regulated expression during postnatal development. *Gene*, 214(1-2), 121-129.
49. Jin, J. P., & Chong, S. M. (2010). Localization of the two tropomyosin-binding sites of troponin T. *Arch Biochem Biophys*, 500(2), 144-150.
50. Jin, J. P., Chong, S. M., & Hossain, M. M. (2007). Microtiter plate monoclonal antibody epitope analysis of Ca²⁺- and Mg²⁺-induced conformational changes in troponin C. *Arch Biochem Biophys*, 466(1), 1-7.
51. Jin, J. P., Huang, Q. Q., Yeh, H. I., & Lin, J. J. C. (1992). Complete Nucleotide-Sequence and Structural Organization of Rat Cardiac Troponin-T Gene - a Single Gene Generates Embryonic and Adult Isoforms Via Developmentally Regulated Alternative Splicing. *J Mol Biol*, 227(4), 1269-1276.
52. Jin, J. P., & Lin, J. J. C. (1988). Rapid Purification of Mammalian Cardiac Troponin-T and Its Isoform Switching in Rat Hearts during Development. *Journal of Biological Chemistry*, 263(15), 7309-7315.
53. Jin, J. P., & Root, D. D. (2000). NH₂-terminal variable region-based modulation of conformation and flexibility of troponin T: A fluorescence spectral study. *Biophys J*, 78(1), 365a-365a.
54. Jin, J. P., & Smillie, L. B. (1994). An Unusual Metal-Binding Cluster Found Exclusively in the Avian Breast Muscle Troponin-T of Galliformes and Craciformes. *FEBS Lett*, 341(1), 135-140.

55. Jin, J. P., & Wang, K. (1991). Nebulin as a Giant Actin-Binding Template Protein in Skeletal-Muscle Sarcomere - Interaction of Actin and Cloned Human Nebulin Fragments. *FEBS Lett*, 281(1-2), 93-96.
56. Leavis, P. C., & Gergely, J. (1984). Thin Filament Proteins and Thin Filament-Linked Regulation of Vertebrate Muscle-Contraction. *Crc Critical Reviews in Biochemistry*, 16(3), 235-305.
57. Lin, J. J., Chou, C. S., & Lin, J. L. (1985). Monoclonal antibodies against chicken tropomyosin isoforms: production, characterization, and application. *Hybridoma (Larchmt)*, 4(3), 223-242.
58. Linke, W. A., Ivemeyer, M., Labeit, S., Hinssen, H., Ruegg, J. C., & Gautel, M. (1997). Actin-titin interaction in cardiac myofibrils: probing a physiological role. *Biophys J*, 73(2), 905-919.
59. Mak, A. S., & Smillie, L. B. (1981). Structural interpretation of the two-site binding of troponin on the muscle thin filament. *J Mol Biol*, 149(3), 541-550.
60. Marieb, E. N., & Hoehn, K. (2013). *Human anatomy & physiology* (9th ed.). Boston: Pearson.
61. Maruyama, K., & Ebashi, S. (1965). Alpha-Actinin a New Structural Protein from Striated Muscle .2. Action on Actin. *J Biochem*, 58(1), 13-19.
62. Meinrenken, W. (1969). [Calcium ion-independent contraction and ATPase in glycerinated muscle fibers following alkaline extraction of troponin]. *Pflugers Arch*, 311(3), 243-255.
63. Mesnard, L., Logeart, D., Taviaux, S., Diriong, S., Mercadier, J. J., & Samson, F. (1995). Human Cardiac Troponin-T - Cloning and Expression of New Isoforms in the Normal and Failing Heart. *Circ Res*, 76(4), 687-692.

64. Mihashi, K. (1972). Organized Interaction of Muscle Proteins .1. Internal Freedom of Tropomyosin in Complex of Troponin-Tropomyosin-F-Actin. *J Biochem*, 71(1), 91-97.
65. Moncman, C. L., & Wang, K. (1995). Nebulette: a 107 kD nebulin-like protein in cardiac muscle. *Cell Motil Cytoskeleton*, 32(3), 205-225.
66. Morris, E. P., & Lehrer, S. S. (1984). Troponin-tropomyosin interactions. Fluorescence studies of the binding of troponin, troponin T, and chymotryptic troponin T fragments to specifically labeled tropomyosin. *Biochemistry*, 23(10), 2214-2220.
67. Nakamura, S., Yamamoto, K., Hashimoto, K., & Ohtsuki, I. (1981). Effect of Chymotryptic Troponin-T Subfragments on the Ca^{2+} Sensitivity of Super-Precipitation. *J Biochem*, 89(5), 1639-1641.
68. Nakaoka, Y. (1972). Effects of Tropomyosin, Troponin and Ca^{2+} on Interaction between F-Actin and Heavy Meromyosin. *Biochim Biophys Acta*, 267(3), 558-567.
69. Nishii, K., Morimoto, S., Minakami, R., Miyano, Y., Hashizume, K., Ohta, M., Shibata, Y. (2008). Targeted disruption of the cardiac troponin T gene causes sarcomere disassembly and defects in heartbeat within the early mouse embryo. *Dev Biol*, 322(1), 65-73.
70. Ogut, O., Granzier, H., & Jin, J. P. (1999). Acidic and basic troponin T isoforms in mature fast-twitch skeletal muscle and effect on contractility. *American Journal of Physiology-Cell Physiology*, 276(5), C1162-C1170.
71. Ogut, O., Hossain, M. M., & Jin, J. P. (2003). Interactions between nebulin-like motifs and thin filament regulatory proteins. *J Biol Chem*, 278(5), 3089-3097.
72. Ogut, O., & Jin, J. P. (1996). Expression, zinc-affinity purification, and characterization of a novel metal-binding cluster in troponin T: metal-stabilized alpha-helical structure and effects of the NH_2 -terminal variable region on the conformation of intact troponin T

- and its association with tropomyosin. *Biochemistry*, 35(51), 16581-16590.
73. Pan, B. S., Gordon, A. M., & Potter, J. D. (1991). Deletion of the first 45 NH₂-terminal residues of rabbit skeletal troponin T strengthens binding of troponin to immobilized tropomyosin. *J Biol Chem*, 266(19), 12432-12438.
 74. Pan, B. S., & Potter, J. D. (1992). Two genetically expressed troponin T fragments representing alpha and beta isoforms exhibit functional differences. *J Biol Chem*, 267(32), 23052-23056.
 75. Pearlstone, J. R., Carpenter, M. R., & Smillie, L. B. (1977). Primary structure of rabbit skeletal muscle troponin-T. Purification of cyanogen bromide fragments and the amino acid sequence of fragment CB2. *J Biol Chem*, 252(3), 971-977.
 76. Pearlstone, J. R., & Smillie, L. B. (1982). Binding of Troponin-T Fragments to Several Types of Tropomyosin Sensitivity to Ca²⁺ in the Presence of Troponin-C. *Journal of Biological Chemistry*, 257(18), 587-592.
 77. Pfuhl, M., & Pastore, A. (1995). Tertiary structure of an immunoglobulin-like domain from the giant muscle protein titin: a new member of the I set. *Structure*, 3(4), 391-401.
 78. Potter, J. D., & Gergely, J. (1974). Troponin, tropomyosin, and actin interactions in the Ca²⁺ regulation of muscle contraction. *Biochemistry*, 13(13), 2697-2703.
 79. Rief, M., Gautel, M., Schemmel, A., & Gaub, H. E. (1998). The mechanical stability of immunoglobulin and fibronectin III domains in the muscle protein titin measured by atomic force microscopy. *Biophys J*, 75(6), 3008-3014.
 80. Rupp, H. (1983). The Determinants of the Calcium-Dependent Activation of Myofibrils from Rat-Heart as Judged by Myofibrillar Adenosine-Triphosphatase and Superprecipitation of Natural Actomyosin. *Molecular Physiology*, 3(5-6), 249-263.
 81. Sanger, J. W., & Sanger, J. M. (2001). Fishing out proteins that bind to titin. *Journal of*

- Cell Biology*, 154(1), 21-24.
82. Schachat, F. H., Diamond, M. S., & Brandt, P. W. (1987). Effect of Different Troponin T-Tropomyosin Combinations on Thin Filament Activation. *J Mol Biol*, 198(3), 551-554.
 83. Sheng, J. J., & Jin, J. P. (2014). Gene regulation, alternative splicing, and posttranslational modification of troponin subunits in cardiac development and adaptation: a focused review. *Front Physiol*, 5, 165.
 84. Smillie, L. B. (1982). Preparation and identification of alpha- and beta-tropomyosins. *Methods Enzymol*, 85 Pt B, 234-241.
 85. Spudich, J. A., Huxley, H. E., & Finch, J. T. (1972). Regulation of Skeletal-Muscle Contraction .2. Structural Studies of Interaction of Tropomyosin-Troponin Complex with Actin. *J Mol Biol*, 72(3), 619-632.
 86. Spudich, J. A., & Watt, S. (1971). Regulation of Rabbit Skeletal Muscle Contraction .1. Biochemical Studies of Interaction of Tropomyosin-Troponin Complex with Actin and Proteolytic Fragments of Myosin. *Journal of Biological Chemistry*, 246(15), 4866-&.
 87. Studier, F. W., & Moffatt, B. A. (1986). Use of Bacteriophage-T7 Rna-Polymerase to Direct Selective High-Level Expression of Cloned Genes. *J Mol Biol*, 189(1), 113-130.
 88. Takeda, S., Yamashita, A., Maeda, K., & Maeda, Y. (2003). Structure of the core domain of human cardiac troponin in the Ca⁽²⁺⁾-saturated form. *Nature*, 424(6944), 35-41.
 89. Vale, R. D., & Milligan, R. A. (2000). The way things move: looking under the hood of molecular motor proteins. *Science*, 288(5463), 88-95.
 90. Vaneerd, J. P., & Kawasaki, Y. (1973). Effect of Calcium(Ii) on Interaction between Subunits of Troponin and Tropomyosin. *Biochemistry*, 12(24), 4972-4980.

91. Verin, A. D., & Gusev, N. B. (1988). Role of the N-Terminal Fragment of Troponin-T in the Interaction with Components of the Heart Troponin-Tropomyosin Complex. *Biochemistry-Moscow*, 53(8), 1071-1081.
92. Veselka, J. (2012). *Cardiomyopathies - From Basic Research to Clinical Management*. (CC BY 3.0 License)
93. Vinogradova, M. V., Stone, D. B., Malanina, G. G., Karatzaferi, C., Cooke, R., Mendelson, R. A., & Fletterick, R. J. (2005). Ca⁽²⁺⁾-regulated structural changes in troponin. *Proc Natl Acad Sci U S A*, 102(14), 5038-5043.
94. Volkmann, N., & Hanein, D. (2000). Actomyosin: law and order in motility. *Curr Opin Cell Biol*, 12(1), 26-34.
95. Wang, J., & Jin, J. P. (1997). Primary structure and developmental acidic to basic transition of 13 alternatively spliced mouse fast skeletal muscle troponin T isoforms. *Gene*, 193(1), 105-114.
96. Wang, J., & Jin, J. P. (1998). Conformational modulation of troponin T by configuration of the NH₂-terminal variable region and functional effects. *Biochemistry*, 37(41), 14519-14528.
97. Wang, K., McClure, J., & Tu, A. (1979). Titin: major myofibrillar components of striated muscle. *Proc Natl Acad Sci U S A*, 76(8), 3698-3702.
98. Wang, K., & Wright, J. (1988). Architecture of the sarcomere matrix of skeletal muscle: immunoelectron microscopic evidence that suggests a set of parallel inextensible nebulin filaments anchored at the Z line. *Journal of Cell Biology*, 107(6 Pt 1), 2199-2212.
99. Watkins, H., Seidman, C. E., Seidman, J. G., Feng, H. S., & Sweeney, H. L. (1996). Expression and functional assessment of a truncated cardiac troponin T that causes hypertrophic cardiomyopathy - Evidence for a dominant negative action. *Journal of*

Clinical Investigation, 98(11), 2456-2461. doi: Doi 10.1172/Jci119063

100. Wei, B., & Jin, J. P. (2011). Troponin T isoforms and posttranscriptional modifications: Evolution, regulation and function. *Arch Biochem Biophys*, 505(2), 144-154.
101. Yamamoto, K., & Maruyama, K. (1973). Interaction of Troponin-I and Tropomyosin. *J Biochem*, 73(5), 1111-1114.
102. Zhang, Z., Biesiadecki, B. J., & Jin, J. P. (2006). Selective deletion of the NH₂-terminal variable region of cardiac troponin T in ischemia reperfusion by myofibril-associated mu-calpain cleavage. *Biochemistry*, 45(38), 11681-11694.
103. Zot, A. S., & Potter, J. D. (1987). Structural Aspects of Troponin-Tropomyosin Regulation of Skeletal-Muscle Contraction. *Annual Review of Biophysics and Biophysical Chemistry*, 16, 535-559.

ABSTRACT**THE NH₂-HYPERVARIABLE REGION MODULATES THE BINDING AFFINITY OF TROPONIN T FOR TROPOMYOSIN**

by

CHINTHAKA KAUSHALYA AMARASINGHE**December 2014****Advisor:** Jian-Ping Jin, M.D., Ph.D.**Major:** Physiology**Degree:** Master of Science

The troponin complex plays a central role in the allosteric function of sarcomeric thin filaments by enacting conformational changes during the Ca²⁺-regulated contraction and relaxation of striated muscle. The troponin subunit T (TnT) has two binding sites for tropomyosin (Tm) and is responsible for anchoring the troponin complex to the thin filament. Although the C-terminal and middle regions of the TnT polypeptide chain are highly conserved among the three muscle type isoforms, the hypervariable N-terminal region has evolutionarily diverged significantly among isoforms. Previous studies have shown that the N-terminal variable region fine-tunes Ca²⁺ regulation of muscle contractility via modulation of the overall molecular conformation of TnT, and its interactions with Tm. In the present study, intact TnT and representative TnT fragments were engineered, and expressed in *E. coli*. The TnT proteins were then purified using various biochemical and chromatographic techniques and prepared for functional studies. Tropomyosin binding affinity was analyzed using solid phase protein binding assays to investigate the modulatory effects of the N-terminal variable region. The results demonstrated that in the absence of the N-terminal variable region, TnT's conserved middle region and C-terminal T2 region Tm-binding sites showed comparable Tm-binding affinities across isoforms. The data demonstrate that without the modulatory effect of the N-

terminal variable region, the intrinsic Tm-binding affinities of the two sites are both high. In contrast, the presence of the isoform specific N-terminal variable region differentially reduces the binding affinity of TnT for Tm, primarily at the middle region binding site. These novel findings indicate that the N-terminal variable region plays a key role in the functional difference of muscle fiber type-specific, developmental, splice variant, and pathogenic TnT isoforms by modulating the interactions with Tm during the contraction and relaxation of cardiac and skeletal muscle.

AUTOBIOGRAPHICAL STATEMENT

CHINTHAKA KAUSHALYA AMARASINGHE

EDUCATION

- 2014 MS in Physiology, Wayne State University School of Medicine, Detroit, MI
 2012 BS in Neuroscience, University of Michigan, Ann Arbor, MI

EXPERIENCE

Laboratory Assistant – Brenner Lab, University of Michigan Hospital (2010-2012)

Identified natural compounds found in specific diets (such as Mediterranean diet) that may increase the expression of BRCA1 protein. BRCA1 is a protein involved in DNA repair which is expressed in the cells of breast and other tissue

Laboratory Assistant – Tesmer Lab, University of Michigan, Ann Arbor, MI (2010)

Prepared protein gels for electrophoresis and other laboratory solutions and buffers

SERVICE

- 2013-present Volunteer-Cass Clinic (Conduct patient interviews, take vitals, lifestyle counseling, and presenting cases to physician on site.)
 2013-present Volunteer-Detroit Receiving Hospital (5M Telemetry unit, answer unit phone calls and assist nurses and patients)
 2013-present Tutor-Detroit Public Library “Detroit Reads!” (Mentor and teach adults math and reading skills and help them prepare for the GED)
 2013 Judge-Wayne State University, Annual Summer Undergraduate Research Joint Mini Symposium
 2013 Volunteer-Evergreen Academy (Talked to senior high school students about higher education opportunities)
 2011-2012 Active Member-University of Michigan Pre-Med Club (Participated in fundraising, volunteer events and Make-A-Wish foundation events)
 2010-2012 Volunteer-University of Michigan Hospital (Unit host at the Cardiovascular Center Intensive Care Unit)

ABSTRACTS

1. Madhuri Kakarala, Shiv K. Dubey, Craig J. Dobry, Xinjian Peng, Genoveva Murillo, Satyam R. Parikh, **Chinthaka Amarasinghe**, Rajendra Mehta, and Dean E. Brenner. Vitamin D compounds induce BRCA1 expression and inhibit breast stem cells. In: Proceedings of the 102nd Annual Meeting of the American Association for Cancer Research; 2011 Apr 2-6; Orlando, FL. Philadelphia (PA): AACR; Cancer Res 2011;71(8 Suppl):Abstract nr 1842. doi:10.1158/1538-7445.AM2011-1842